Optimizing Mixtures of Metal–Organic Frameworks for Robust and Bespoke Passive Atmospheric Water Harvesting

Harriman, Charles; Ke, Qia; Vlugt, Thijs J.H.; Howarth, Ashlee J.; Simon, Cory M.

DOI
10.1021/acsengineeringau.5c00051

Publication date
2025

Document Version
Final published version

Published in
ACS Engineering Au

Citation (APA)
Harriman, C., Ke, Q., Vlugt, T. J. H., Howarth, A. J., & Simon, C. M. (2025). Optimizing Mixtures of Metal–Organic Frameworks for Robust and Bespoke Passive Atmospheric Water Harvesting. *ACS Engineering Au*, *5*(6), 707-725. https://doi.org/10.1021/acsengineeringau.5c00051

ACS ENGINEERING Au
AN OPEN ACCESS JOURNAL OF THE AMERICAN CHEMICAL SOCIETY

pubs.acs.org/engineeringau
Article

Optimizing Mixtures of Metal–Organic Frameworks for Robust and Bespoke Passive Atmospheric Water Harvesting

Charles Harriman, Qia Ke, Thijs J. H. Vlugt,* Ashlee J. Howarth,* and Cory M. Simon*

Cite This: ACS Eng. Au 2025, 5, 707–725
Read Online

ABSTRACT: Atmospheric water harvesting (AWH) is a method to obtain clean water in remote or underdeveloped regions including, but not limited to, those with an arid or desert climate. For passive (i.e., relying on ambient cooling and, for heating, natural sunlight—as opposed to an external power source), adsorbent-based AWH, an adsorbent bed is employed to capture water from cold, humid air at nighttime, while during the daytime the bed is then exposed to natural sunlight to heat it and desorb the water for collection. Metal–organic frameworks (MOFs) are tunable, nanoporous materials with suitable water adsorption properties for comprising this adsorbent bed. The water delivery by the MOF adsorbent bed in a passive AWH device depends on (1) the nighttime, capture conditions (temperature and humidity) and daytime, release conditions (temperature, humidity, and solar flux) and (2) the structure(s) of the MOF(s) comprising the bed, which dictate MOF-water interactions. Notably, the capture and release conditions vary from region-to-region and season-to-season and fluctuate from day-to-day, while different MOFs offer different water adsorption isotherms. Consequently, we propose (1) comprising the adsorbent bed for passive AWH with a *mixture* of MOFs and (2) tailoring this MOF mixture to particular geographic regions and time frames. We hypothesize each MOF in the mixture can specialize in delivering water under different capture and release conditions, ensuring the adsorbent bed delivers adequate water on every day—despite fluctuations in temperature, humidity, and solar flux. Herein, we develop an optimization framework to determine the total mass and composition of a MOF mixture for comprising a bespoke (i.e., tailored to a declared geographic region and time frame) adsorbent bed for robust (i.e., delivering adequate water every day) passive AWH. We combine weather data in the declared region, equilibrium water adsorption data in the candidate MOFs, and thermodynamic water adsorption models (as a simplifying assumption, we neglect heat and water transfer limitations) to frame a linear program expressing our optimal design principle: adjust the mass of each candidate MOF comprising the adsorbent bed to minimize mass (important for portability and a proxy for cost) while satisfying daily water delivery constraints. Based on case studies in the Chihuahuan and Sonoran Deserts, we find (1) a mixed-MOF adsorbent bed can be, but is not always, lighter (e.g., ≈40% lighter) than the optimized single-MOF counterpart; and (2) the optimal composition and mass of the adsorbent bed differ by both geographic region and time frame. Finally, we visualize the linear program for a reduced problem with a two-dimensional design space to gain intuition, conduct a sensitivity analysis, and compare to an AWH field study. Our work is a starting point for optimizing the composition of bespoke adsorbent beds for robust, passive AWH.

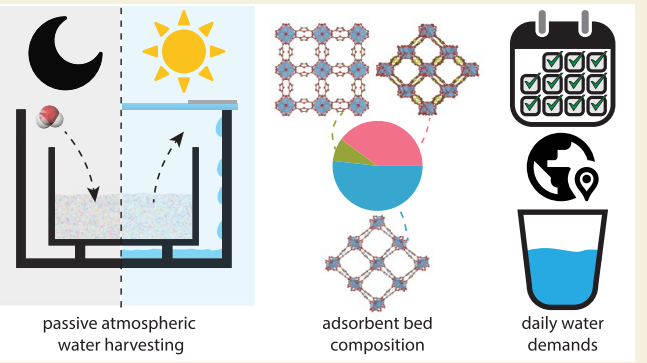

KEYWORDS: *atmospheric water harvesting, metal–organic frameworks, optimization, linear programming, MOF mixtures*

1. INTRODUCTION

1.1. Water Scarcity

Freshwater for agricultural (irrigation, livestock, aquaculture, etc.), municipal/domestic (drinking, cooking, bathing, washing clothes and dishes, etc.), and industrial (manufacturing a product, washing, cooling, cleaning, etc.) activities is crucial for human health, prosperity, and well-being.[1] Conventionally, humans obtain freshwater from rainfall, underground aquifers, rivers, and lakes.[2] The local supply of blue water (fresh surface- and ground-water)[3] from conventional sources, however, is often insufficient for local demand. Problematically, ∼7/10 of the global population experience blue water scarcity for at least one month of the year.[4] By definition, blue water scarcity means the blue water footprint (fresh surface- or ground-water withdrawn then incorporated into a product or evaporated) in that region exceeds availability.[4] Water pollution,[5] population

Received: June 19, 2025
Revised: October 18, 2025
Accepted: October 21, 2025
Published: November 3, 2025

growth,[6] and climate change[7] are worsening water scarcity in many regions.

Approaches to alleviate water scarcity include conserving water, making water-use more efficient, and increasing the supply of clean water.[1] Water conservation requires difficult behavioral changes. Improving water-use efficiency requires costly infrastructure upgrades. Both still may be insufficient to alleviate water scarcity in arid regions.[8] Approaches to increase the supply of clean water include building or expanding reservoirs, desalinating seawater, and recycling wastewater. All rely on a water transportation network and impose high infrastructure costs. Moreover, particularly, reservoirs impact ecosystems; desalinating seawater is energy-intensive and requires access to the ocean/sea; and recycling wastewater is unpalatable to many.[2,9−13] Consequently, expanding water supply in poor, underdeveloped, and/or landlocked regions distant from natural water sources is challenging.[11,14]

1.2. Atmospheric Water Harvesting

Atmospheric water harvesting (AWH) entails the direct capture and collection of water vapor from the air.[15] Earth's atmosphere is an untapped, ubiquitous, abundant source of clean water.[14,15] Interestingly, some biological species—including beetles,[16] grass,[17] cacti,[18] and moss[19] in the desert—exhibit surface-structures and -chemistries that promote the nucleation of water droplets from fog or humid air to collect water for drinking, storage, or irrigation;[20] likewise, spider webs can collect water from humid air, thanks to hydrophilic nanofibrils on spider silk.[21] Analogously, (often, bioinspired[22]) engineered technologies for AWH could provide quality, clean water at the point-of-use in arid or semiarid regions where conventional methods to increase water supply fail: e.g., for low-income households and communities in underdeveloped or remote regions lacking water transportation infrastructure and/or an electrical grid.[15] Moreover, AWH is applicable for emergency use after a natural disaster that disrupts water supply and for remote military operations.[23] AWH methods[14,15,24−28] include harvesting fog via a spiderweb-like mesh of material,[29−31] condensing water vapor onto a cold surface (dewing),[32−34] and adsorbing water from air into porous materials.[35−48] From a standpoint of energy input, AWH technologies can be *passive*, utilizing natural or ambient energy sources (e.g., sunlight for heating or underground soil for cooling), or *active*, requiring e.g., an electrical power source.[14,27]

AWH via porous materials functioning as water adsorbents offers several advantages over dewing and mesh-based fog harvesting. First, adsorbent-based AWH is more climate- and thus region-versatile. As adsorbents can capture water from air with as low as ≈10% relative humidity,[35,49] adsorbent-based AWH can function even in arid or desert climates with infrequent fog formation. Second, the adsorbed water can be released from the adsorbent using heat from natural sunlight, enabling a passive AWH technology that functions off-electrical-grid. Note, adsorption-based AWH can also be active, then providing multiple adsorption−desorption cycles per day instead of just one.[49,50] Third, modular and scalable designs of adsorbent-based AWH devices[51−54] could provide portable and personal-scale to stationary and community-scale[55] AWH units.

Among many categories of adsorbents investigated for passive AWH,[27,45] including polymeric hydrogels,[56] salts, silica gels, zeolites,[52] and covalent organic frameworks (COFs),[57,58] metal−organic frameworks (MOFs) stand out—largely, due to their favorable water adsorption properties.[44,59−64] MOFs are crystalline materials composed of organic linker molecules coordinated with metal ions, chains, or clusters. MOFs exhibit nanosized pores with large internal surface areas decorated with chemical functionalities, endowing them with the capability to adsorb water from air.[65] Box 1 explains the working principle of a MOF-based passive AWH device, while Figure 1 shows a schematic of its diurnal water capture-then-release cycle and an example water delivery calculation. MOFs can display temperature-sensitive, sigmoid- or step-shaped (arising from cooperative water adsorption[49]), and low-hysteresis water adsorption isotherms. (See Figure 1.) These water adsorption properties allow a MOF to function as a reversible water-capture ↔ water-release switch in response to relatively small night ↔ day temperature and humidity changes.[49,63,66,67] Consequently, MOFs can exhibit a high water deliverable capacity (hereafter, *water delivery*) under a passive adsorption (night)—desorption (day) cycle for AWH. For a MOF to function as a switch and achieve a high water delivery on a given day, its [temperature-dependent] water adsorption step must lie at a lower relative humidity than nighttime air and at a higher relative humidity than daytime air under sun exposure. So, different MOFs, with different relative humidities at which their water adsorption switch is triggered, provide different water deliveries in different climates and weather. Because MOF structures are modular and tunable,

Box 1

A passive AWH device that leverages a metal−organic framework (MOF) to capture water from the air constitutes an outer case, with a cover, containing an open box holding MOF powder. At nighttime, the case is held open to expose the MOF to the air. The MOF adsorbs water from the (relative to daytime air, typically) cold and humid nighttime air to [hopefully] fill its pores with water. The case is then closed. At daytime, the closed case is exposed to sunlight, which heats the MOF powder and drives desorption of water out of the MOF. The desorbed water condenses on the inner walls of the outer-case, which are cooler thanks to reflectors on the periphery of the cover.[49,75] The frequency of water delivery by a passive AWH device is once per day (nighttime: adsorption/capture; daytime: desorption/release). See Figure 1. The MOF powder, provided the MOF exhibits high hydrolytic and architectural stability,[50] can be reused each day.

The *water delivery* of the harvester on a given day is the amount of water captured by the MOF bed at nighttime minus the water retained in the MOF bed at daytime, under solar irradiation—assuming all of the water desorbed from the MOF is condensed and recovered. The water delivery depends on (1) the structure/composition of the MOF bed; (2) last night's temperature and humidity; and (3) this day's temperature, humidity, and solar flux. Depending on the stability of the MOF, the water delivery may depend on the adsorption−desorption cycle number, too.[50] In addition to equilibrium water adsorption in the MOF, both heat and water transfer rates in the MOF, and, thus, the geometry of the MOF granules and bed, affect the water delivery.[46,76,77] The modeling and design of MOF-based AWH devices at various scales is an active area of research.[37,61,78−84]

https://doi.org/10.1021/acsengineeringau.5c00051
ACS Eng. Au 2025, 5, 707−725

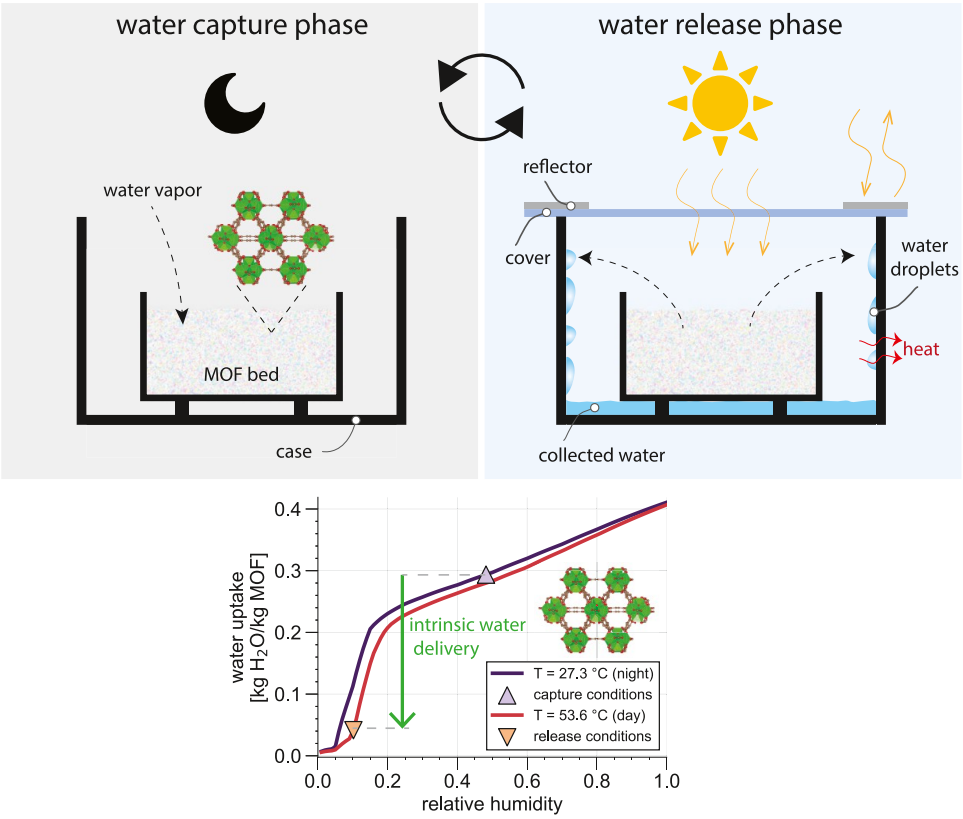

Figure 1. Working principle of a passive, MOF-based atmospheric water harvester, (top) which operates over a diurnal cycle and (bottom) whose performance is described by the water delivery. (Heavily inspired by ref 75)

many MOFs with diverse pore sizes and shapes and internal surface chemistries have been reported;[68,69] advantageously, we can pick MOF(s) for the AWH adsorbent bed whose water adsorption properties are tailored to passive AWH in particular regions and time frames (i.e., climates or weather). N.b., both pore geometry and surface functional groups influence water adsorption in a MOF.[63,70−72] Finally, many MOFs are water-stable, granting them with good adsorption−desorption cyclability and preventing components of the MOF from leaching into and contaminating the water they deliver.[60,73,74]

1.3. Our Contribution: Optimizing the Composition of a Mixed-MOF Adsorbent Bed for Robust, Bespoke Passive AWH

Herein, we develop and demonstrate a workflow to optimally design the composition of a MOF mixture comprising an adsorbent bed for passive AWH.

We incorporate three key principles into our definition of the optimal design of an adsorbent bed for passive AWH. First, we wish for the adsorbent bed to be as light (i.e., minimal mass) as possible. For portable harvesters, this is essential. Even for stationary harvesters, the cost is likely correlated with the total mass of MOF needed. Second, *bespokeness*: the composition of the adsorbent bed should be tailored to the particular geographic region and time frame (e.g., season) wherein the AWH device will operate.[49,79] We achieve this by considering the anticipated weather conditions therein. Third, *robustness*: the adsorbent bed should deliver adequate water to satisfy the demand for drinking water on every day of the AWH mission—despite variance in nighttime and daytime temperature and humidity. We achieve this by imposing constraints on the daily water delivery of the adsorbent bed.

A key idea we put forward in the framing of this design problem is that adopting a *mixture* of MOFs, as opposed to a single MOF, to comprise an adsorbent bed for robust passive AWH can be advantageous (i.e., allow for lighter adsorbent beds). To explain, the intrinsic water delivery (kg H_2O delivered per kg MOF, an intrinsic property of the MOF) by a given MOF on a given day depends on both (1) the weather that day, which sets the thermodynamic conditions of the air in the water harvester during the process of (a) water capture at nighttime under ambient conditions and (b) water release at daytime under solar irradiation and (2) the structure and chemistry of the MOF, which dictate its interactions with and, thus, adsorption of water at these thermodynamic conditions. Consequently, the ranking of a candidate set of MOFs according to their intrinsic water delivery differs by (a) region, on the same day, and (b) day of the year, in the same region. As a result, the daily extrinsic water delivery (total kg H_2O delivered by the entire bed, dependent on both its composition and size) by an adsorbent bed comprised of a *mixture* of MOFs may be more robust to the day-to-day variability in weather conditions than a single-MOF bed. Intuitively, each MOF in the mixture can *specialize* in delivering water under specific categories of day/night conditions over the AWH mission. For example, consider an A/B MOF mixture where MOF A exhibits a step in its water adsorption isotherm at a high relative humidity, while the step of MOF B is at a low relative humidity. Then, on a dry and warm night, MOF B will still capture water while MOF A fails to do so. On the other hand, on a humid and cool day, MOF A will still desorb its water while MOF B retains its water. I.e., on a day MOF A (B) fails to deliver water, the MOF B (A) serves as a back-up to ensure

https://doi.org/10.1021/acsengineeringau.5c00051
ACS Eng. Au 2025, 5, 707−725

an adequate amount of water is still delivered. By this mechanism, a mixture of MOFs can grant the water delivery of an adsorbent bed with more robustness to day-to-day weather variability. From another perspective, more simply: allowing for *mixtures* of MOFs grants us greater design flexibility for tuning the water adsorption of the adsorbent bed as a function of temperature and relative humidity. Relatedly, adsorbent mixtures have been proposed for packed beds for gas separations to combine favorable properties of multiple adsorbents; a process model showed a dual adsorbent could extend the purity-recovery Pareto front achievable by a single-adsorbent process.[85]

(Note, a mixed-MOF adsorbent bed for AWH could be realized by (i) mixing together the powders of the distinct MOFs synthesized independently; (ii) a one-pot synthesis resulting in mixed-MOF phases;[86] or (iii) holding the powders of distinct MOFs in separate compartments of the AWH device).

We formulate the problem of designing the optimal composition of a bespoke adsorbent bed for robust passive AWH as a linear program.[87] The decision variables are the masses of the candidate MOFs that comprise the adsorbent bed. The objective function to minimize is the total mass of the MOF adsorbent bed. (Trivially, we may modify the objective function to instead express the total monetary cost of the adsorbent bed by introducing the cost [$/kg] of each MOF.) The list of [hard] constraints impose that a specified amount of water, at least, must be delivered on each day of the AWH mission. Two data sets inform the optimization problem: (1) forecasted or historical time series data of the air temperature, humidity, and land surface temperature (reflective of the solar flux) in the region over the time frame; and (2) experimentally measured, equilibrium water adsorption isotherms in the candidate MOFs. In conjunction with thermodynamic models of water adsorption (e.g., Polanyi adsorption theory[88]), these data allow us to predict the intrinsic water delivery by each MOF structure on each day of the AWH mission and, thus, optimize the composition of the MOF bed for the particular region and time frame. (Note, for a higher-fidelity prediction of the water delivery by an adsorbent bed, one could also model[37,79] the kinetics of heat and water transfer in the MOFs[77,89] as well as adsorptive competition with water from other gas species in the air such as carbon dioxide[90,91] (e.g., via real adsorbed solution theory[92−95] and a model for the activity coefficients[96]). However, this would require additional data for each MOF—including the diffusion coefficient and mass transfer coefficient of water, heat of water adsorption,[97] specific heat, thermal conductivity, particle size and shape distribution,[98] and carbon dioxide adsorption isotherms—and knowledge or joint optimization of the geometry of the adsorbent bed).

To illustrate and provide insights, we optimize the composition of a mixed-MOF bed for passive AWH in two distinct desert regions, the Sonoran and Chihuahuan Deserts, over three ten-day periods during the summer. For comprising the MOF bed, we consider a library of eight water-stable MOFs with reported water adsorption isotherms favorable for water harvesting: MOF-801, KMF-1, CAU-23, MIL-160, MOF-303, CAU-10-H, Al-Fum, and MIP-200. We find (1) comprising the adsorbent bed with a *mixture* of MOFs sometimes affords a lighter MOF bed (e.g., ≈40% lighter) than achievable via a single-MOF bed and (2) the optimal composition and total mass of the MOF mixture differ by region and time frame. Our work is a starting point for the data-informed, model-based optimal design of the composition of MOF adsorbent beds for bespoke and robust passive AWH and calls for adoption of MOF mixtures where each MOF specializes to different capture and release conditions.

2. METHODOLOGY FOR OPTIMIZING THE COMPOSITION OF A MIXED-MOF ADSORBENT BED FOR BESPOKE, ROBUST PASSIVE AWH

Our goal is to optimize the composition of an adsorbent bed, comprised of a mixture of MOFs, for a passive atmospheric water harvesting (AWH) mission (a) in a particular geographic region and time frame and (b) under declared daily water delivery demands. The flowchart in Figure 2 presents a high-level guide through our design process.

2.1. Specify the Atmospheric Water Harvesting Mission

First, define the water harvesting mission by specifying a geographic region (e.g., Chihuahuan Desert), a time frame in that region (e.g., June 1−10), and a minimum daily water demand on each day (e.g., 2 kg H_2O/day every day). The water demands, attributed to an individual, team, household, or community, could differ by day. For example, demand for water may be higher on a day forecasted to be hot and involve a high level of physical activity. We denote the time frame, consisting of D days, with a list $[D] := (1, ..., D)$ and the minimum daily water deliveries with a list $\mathbf{q} = (q_1, ..., q_D)$ [kg H_2O].

2.2. Assemble a Library of Candidate MOFs

Next, compile a library of N MOF structures as candidates for comprising the adsorbent bed of the passive AWH device. We denote the MOF candidates as an [arbitrarily ordered] list $[N] := (1, ..., N)$. Criteria for selecting MOFs for the library include water stability and low toxicity.

2.3. Gather Data to Inform the Design of the Adsorbent Bed

To design an optimal mixed-MOF adsorbent bed, we need to predict the water delivery by each MOF on each day of the passive AWH mission. Two data sets inform these predictions: (1) weather time series data in the region and (2) water adsorption data in the MOFs.

2.3.1. Weather Time Series Data. Gather historical or forecasted weather (bulk air temperature and humidity and land surface temperature or solar flux) time series data in the region. E.g., for historical weather data, the US National Oceanic and Atmospheric Administration (NOAA)[99,100] runs a network of climate monitoring stations with high-quality instruments that measure the hourly average temperature and relative humidity of the air and the (land) surface temperature. On the basis of this weather data, predict, on each day $d \in [D]$ of the AWH mission the:

- *Water capture (adsorption) conditions*: the temperature T_d^{night} and relative humidity ϕ_d^{night} of the ambient air during the nighttime.
- *Water release (desorption) conditions*: the temperature T_d^{day} and relative humidity ϕ_d^{day} of the air inside the AWH device while exposed to natural sunlight during the daytime.

We assume the capture (release) conditions are constant over the adsorption (desorption) process—but, not over the mission. Straightforwardly, the capture conditions constitute the temperature and humidity of bulk air during nighttime. By

https://doi.org/10.1021/acsengineeringau.5c00051
ACS Eng. Au 2025, 5, 707−725

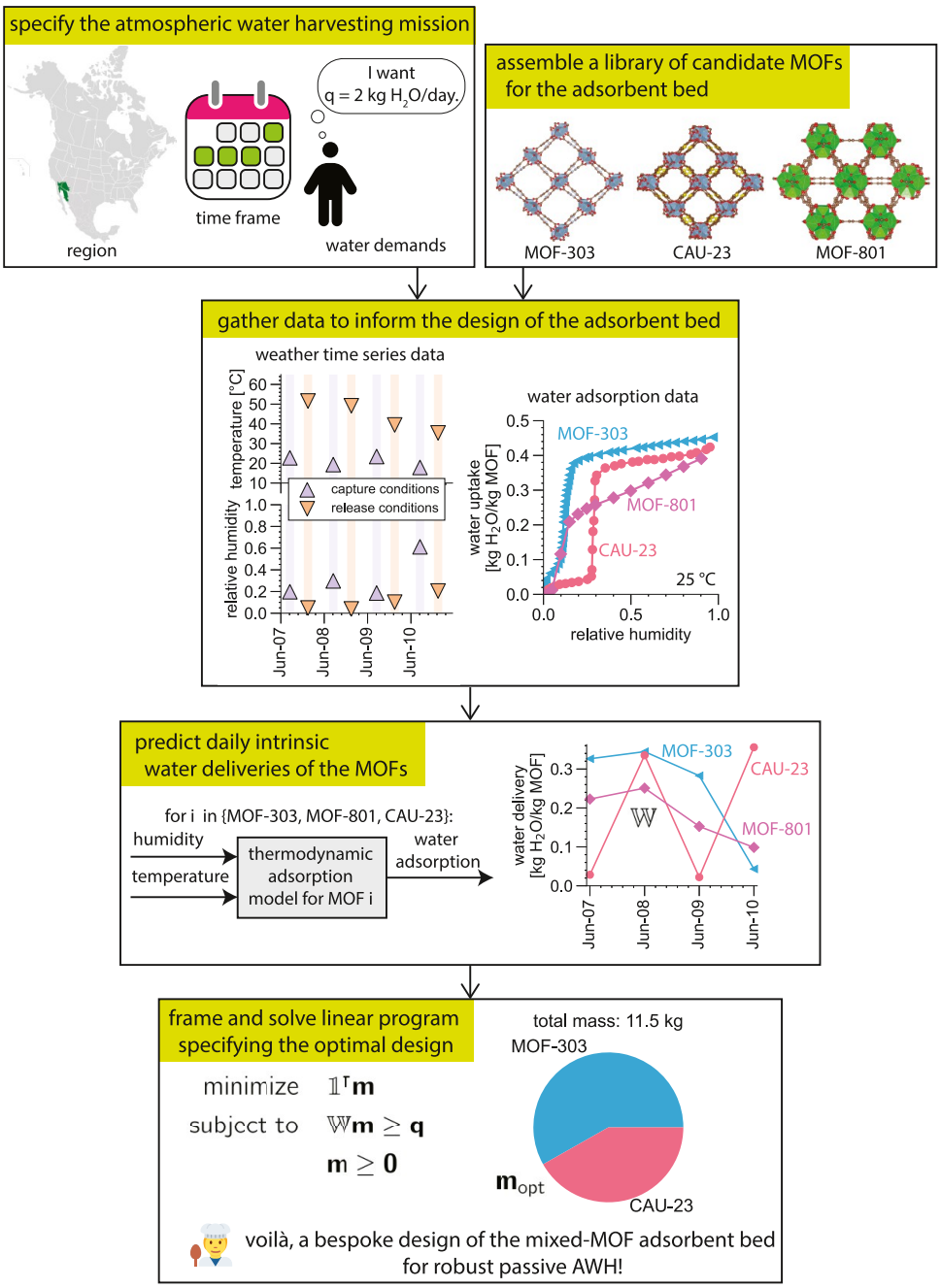

Figure 2. Workflow for designing a bespoke mixed-MOF adsorbent bed for robust passive atmospheric water harvesting, illustrated with a four day mission in the Chihuahuan Desert and three candidate MOFs. (Map reprinted with permission under a Creative Commons CC BY-SA 3.0 from Wikipedia at `commons.wikimedia.org/wiki/File:Sonoran_Desert_map.svg`.).

contrast, for the release conditions, the irradiation of the MOF by natural sunlight raises its temperature above the bulk air during daytime. If the solar flux were available, one could estimate this temperature with knowledge of the MOF's solar reflectance and infrared emissivity.[101] Instead, we adopt the land surface temperature, which correlates with solar flux, as a proxy for the temperature the MOF would reach under solar irradiation.

2.3.2. Water Adsorption Data. Gather or measure equilibrium water adsorption isotherm(s) in each candidate MOF at/near temperature(s) encountered during the AWH mission. (A water adsorption isotherm constitutes a data table giving the amount of water adsorbed in a MOF [kg H_2O/kg MOF] over a list of relative humidities ranging from 0% to 100%—at thermodynamic equilibrium and at a given temperature.) Water adsorption data are needed to build thermodynamic or interpolative models that predict the amount of water adsorbed [kg H_2O/kg MOF] in each MOF at any given temperature and humidity. Of particular interest are the capture and release conditions on each day of the AWH mission. For the highest fidelity predictions of water adsorption, the water adsorption data should densely cover the temperature−humidity space encountered over the AWH mission. However, e.g., for Polanyi adsorption theory,[88] only a single water adsorption isotherm in a MOF is necessary to predict adsorption at different temperatures.

https://doi.org/10.1021/acsengineeringau.5c00051
ACS Eng. Au 2025, 5, 707−725

2.4. Predict Daily Intrinsic Water Deliveries by the MOFs

To decide on the mass of each MOF to put in the adsorbent bed, we predict the intrinsic water delivery by each MOF on each day of the AWH mission.

2.4.1. Build Thermodynamic or Interpolative Models of Water Adsorption in the MOFs. First, we leverage the equilibrium water adsorption data to construct models that predict the intrinsic, equilibrium amount of water adsorbed in each MOF $n \in [N]$, $w^{(n)}$ [kg H_2O/kg MOF], as a function of temperature T and relative humidity ϕ. Generally, this model $w^{(n)}(T, \phi)$ is usually needed because experimentally measured water adsorption is not available at every capture and release condition encountered during the AWH mission. Two routes to construct $w^{(n)}(T, \phi)$ from the water adsorption data are (A) fit a thermodynamic model of water adsorption or (B) interpolation. We include option (C) for high-throughput computational screenings where experimental water adsorption data are unavailable.

2.4.1.1. Simplifying Assumptions. For both parsimony and owing to a lack of data, we make several simplifying [and, arguably, reasonable] assumptions when predicting water adsorption in the MOFs. First, we neglect adsorption−desorption hysteresis that some MOFs (e.g., Y-shp-MOF-5[102]) exhibit. (A fine approximation for the candidate MOFs we selected, whose water adsorption isotherms exhibit negligible hysteresis.) Second, we neglect coadsorption of other gas species in the air, such as carbon dioxide and nitrogen.[90,91] (Likely, a reasonable approximation. H_2O typically adsorbs more strongly and is present at higher concentrations than CO_2 at ambient conditions—compare c.a. 0.04% [by volume] CO_2 with up to c.a. 3% H_2O around room temperature.[91,103−107] Most MOFs require lower-than-ambient temperatures to adsorb significant O_2.[108] Meanwhile, N_2 and Ar are inert so usually adsorb very weakly in MOFs.[91]). Third, we assume the MOF adsorbent bed reaches thermodynamic equilibrium with the air inside the water harvester during the (a) capture and (b) release conditions. Thereby, we neglect the limitations of (i) water transport[77,109,110] and (ii) heat transport[89] in the MOF grains and bed.[37] Regarding water transfer kinetics, it takes some time for, during capture, water molecules to enter a MOF grain and diffuse deep into it and, during release, for water to diffuse out of and exit a MOF grain. Meanwhile, heat transfer kinetics are pertinent to both air-MOF heat transfer and the heat of water ad/desorption. The importance of accounting for heat and water transfer kinetics depends on the size of the MOF grains, the geometry of the adsorbent bed, properties of the MOF (diffusion coefficient, mass transfer coefficient, specific heat capacity, thermal conductivity, etc.), and how long the bed is allowed to ad/desorb water during the capture and release process. (An AWH cycle with MOF-303 powder found it to take ∼150 min for desorption equilibrium and ∼300 min for adsorption equilibrium[77]—matching the time scale for the release and capture process.) Fourth, we assume the MOFs can undergo many water adsorption−desorption and sun exposure cycles without loss in water adsorption capacity. (We handpicked water-stable candidate MOFs; e.g., Al-Fum can undergo thousands of water ad/desorption cycles without measurable loss in water adsorption capacity;[111] MOF-303: > 150).[75]

Relaxing these simplifying assumptions could provide a higher-fidelity prediction of the water delivery by the adsorbent bed. However, these modeling undertakings would require more information/data than currently available: (1) the geometry of the adsorbent bed; (2) the particle size distribution of the MOF granules;[98] (3) more physical properties of the MOFs, including the water diffusion coefficient, water transfer coefficient, specific heat capacity, thermal diffusivity, and water heat of adsorption; (4) adsorption measurements of CO_2, O_2, and N_2 in the MOFs; and (5) the decay in water adsorption in the MOFs over multiple water adsorption−desorption cycles. Finally, good engineering of the AWH device can mitigate heat and mass transfer limitations, anyway.[37,80]

2.4.1.2. Option A: Interpolative Approach. If we possess water adsorption data in a MOF that densely covers the temperature−humidity area pertinent to the AWH mission, [linear, spline, etc.] interpolation can be used to construct the equilibrium water adsorption models $w^{(n)}(T, \phi)$.

2.4.1.3. Option B: Thermodynamic Modeling Approach. If our water adsorption data in a MOF does not densely cover the temperature−humidity area pertinent to the AWH mission, a thermodynamic model is needed to interpolate and extrapolate water adsorption data to construct the water adsorption model $w^{(n)}(T, \phi)$. Among a menu of thermodynamic adsorption models[112] (e.g., Dubinin-Astakhov,[113] dual site Langmuir[114]) to fit to the water adsorption data, we apply Polanyi adsorption theory[88] to construct $w^{(n)}(T, \phi)$.[63,66,115−118] (See Section S1.3.) Polanyi theory is commonly used to model water adsorption in porous materials.[66,115−118] Advantageously, Polanyi theory (1) as a nonparametric model, accommodates complexity in the water adsorption data and (2) allows us to extrapolate a single water adsorption isotherm in a MOF to different temperatures.

2.4.1.4. Option C: Molecular Simulation Or Machine Learning Approach. For a computational screening of a large database of MOFs for water harvesting, one could employ molecular simulations of water adsorption or machine learning models trained on [simulated or experimental] water adsorption data[71,119−124] to predict water adsorption in each MOF at each capture and release condition in the AWH mission.

2.4.2. Daily Intrinsic Water Deliveries. Next, predict the intrinsic water delivery $\Delta w_d^{(n)}$ [kg H_2O/kg MOF] by each MOF $n \in [N]$ on each day $d \in [D]$ of the mission using both (i) the equilibrium water adsorption models $w^{(n)}(T, \phi)$ for $n \in [N]$ and (ii) the predicted capture and release conditions $(T_d^{\text{night}}, \phi_d^{\text{night}})$ and $(T_d^{\text{day}}, \phi_d^{\text{day}})$ for $d \in [D]$. The intrinsic water delivery by a MOF is the intrinsic water uptake in the MOF at the nighttime capture conditions minus the water retained in the MOF at the daytime release conditions:

$$\Delta w_d^{(n)} = \max[0,\ w^{(n)}(T_d^{\text{night}}, \phi_d^{\text{night}}) - w^{(n)}(T_d^{\text{day}}, \phi_d^{\text{day}})] \tag{1}$$

The maximum is needed in the rare case that the MOF delivers zero water because it adsorbs more water during the day than the night (e.g., owing to anomalously high daytime humidity). Because we assume thermodynamic equilibrium and no ad/desorption hysteresis, $\Delta w_d^{(n)}$ is memoryless, i.e., independent of the thermodynamic conditions and thus water adsorption on any previous day. We assemble the intrinsic water delivery by each MOF over each day of the mission in a $D \times N$ matrix $\mathbb{W}$ whose entry (d, n) contains $\Delta w_d^{(n)}$.

https://doi.org/10.1021/acsengineeringau.5c00051
ACS Eng. Au 2025, 5, 707−725

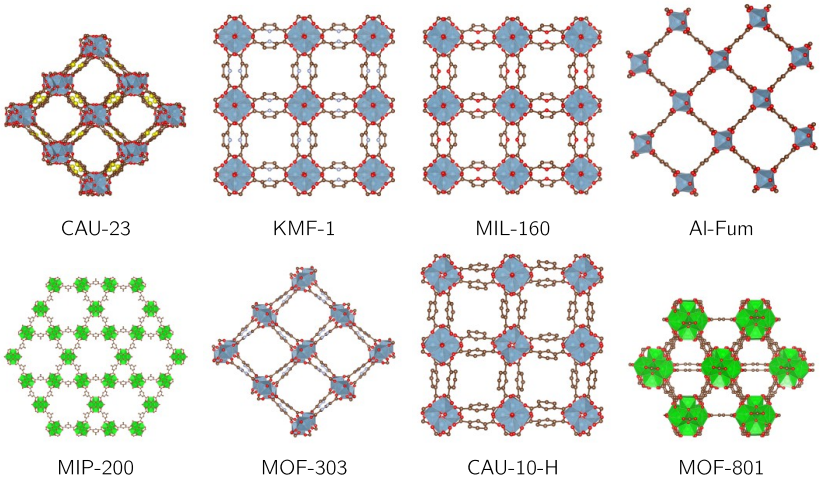

(a) Candidate MOFs.

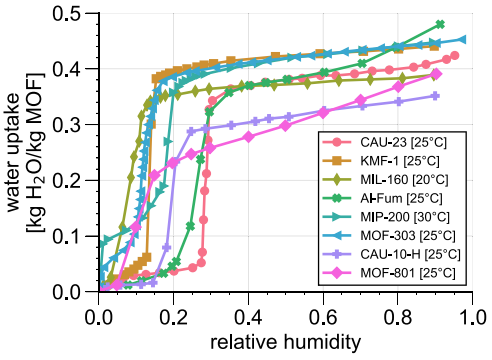

(b) MOF water adsorption data.

Figure 3. Candidate MOF structures for comprising the adsorbent bed of a passive AWH device and their equilibrium water adsorption isotherms. (a) Crystal structures of the candidate MOFs. (MOF-801 from ref 137) (b) Experimentally measured, equilibrium water adsorption isotherms in the candidate MOFs near room temperature. Sources: MOF-801,[35] KMF-1,[128] CAU-23,[129] MIL-160,[130] MOF-303,[132] CAU-10-H,[138] Al-Fum,[111] MIP-200.[136] The raw data are available on our Github repository.

2.5. Frame and Solve a Linear Program Governing the Optimal Design of the Adsorbent Bed

Finally, we formulate then solve an optimization problem expressing our design principles for the composition of the mixed-MOF adsorbent bed for the passive AWH mission: lightness, bespokeness, and robustness.

2.5.1. Decision Variables. The *decision variables* $\mathbf{m} := [m_1, ..., m_N]$ comprise the makeup of the MOF bed, with m_n [kg] the mass of MOF n comprising the bed.

2.5.2. Objective Function. The *objective function* we want to minimize is the total mass of the adsorbent bed [kg MOF]

$$\sum_{n=1}^{N} m_n = \mathbb{1}^{\mathrm{T}}\mathbf{m} \tag{2}$$

First, a light AWH device is desirable for portability. Second, the economic cost of the adsorbent bed is likely to correlate with its total mass.

2.5.3. Constraints. As *hard constraints* (one per day of the mission), we impose that the total water delivered on day d by the MOF bed [kg H_2O] meets or exceeds the demand on that day, q_d [kg H_2O], for every day $d \in [D]$. The constraint for day $d \in [D]$ is

$$\xi \sum_{n=1}^{N} m_n \Delta w_d^{(n)} \geq q_d \tag{3}$$

with $\xi \in [0, 1]$ the fraction of water desorbed from the adsorbent bed that we can condense and recover for use. These constraints impose (1) a bespoke design, as weather data in the region are used to predict the intrinsic water deliveries $\Delta w_d^{(n)}$; (2) water delivery robust to the weather conditions, as adequate [e.g., drinking] water is delivered on every day of the AWH mission, despite varying capture and release conditions.

2.5.4. Linear Program. Putting it all together, the optimal bespoke composition $\mathbf{m}_{\mathrm{opt}}$ of the mixed-MOF bed for robust, passive AWH over the mission follows from solving the linear program[125]

$$\begin{aligned} &\text{minimize } \mathbb{1}^{\mathrm{T}}\mathbf{m} && \text{\# minimize total mass of the MOF bed} \\ &\text{subject to } \xi\mathbb{W}\mathbf{m} \geq \mathbf{q} && \text{\# satisfy demand for water delivery, each day} \\ &\qquad \mathbf{m} \geq \mathbf{0} && \text{\# mass is non-negative} \end{aligned} \tag{4}$$

This linear program has a feasible solution if and only if, on each day, at least one of the candidate MOFs is predicted to deliver nonzero water.

2.5.5. Solving the Linear Program. Finally, we employ an open-source linear program solver such as the `HiGHS`

https://doi.org/10.1021/acsengineeringau.5c00051
ACS Eng. Au 2025, 5, 707−725

solver[126] to obtain the solution to the linear program in eq 4, giving the optimizer $\mathbf{m}_{opt}$ specifying the mass of each MOF constituting the optimal adsorbent bed for the passive AWH device for the mission.

3. RESULTS

As concrete examples of designing a bespoke adsorbent bed for robust passive AWH, we undertake three case studies: (1) Chihuahuan Desert in early June; (2) Sonoran Desert in early June; and (3) Sonoran Desert in middle August. We assume full recovery/collection of the water desorbed from the MOF ($\xi = 1$).

3.1. Candidate MOFs and Their Water Adsorption Isotherms

We propose $N = 8$ MOFs as candidates to comprise the adsorbent bed of a passive AWH device: MOF-801,[127] KMF-1,[128] CAU-23,[129] MIL-160,[130,131] MOF-303,[132] CAU-10-H,[133] Al-Fum,[134,135] and MIP-200.[136] Figure 3a displays the crystal structures of the candidate MOFs. This diverse set of MOFs includes those with Zr(IV) cluster vs Al(III) chain-based nodes and triangular, quadrangular, and hexagonal channel-type pores. We picked these MOFs for (1) displaying water stability, (2) being composed of nontoxic metals, and (3) their experimentally measured water adsorption isotherms (a) being available in the literature and (b) showing minimal adsorption−desorption hysteresis.

Figure 3b displays experimentally measured, equilibrium water adsorption isotherms (near room temperature, 20 to 30 °C) in each candidate MOF. We extracted this data from plots in the literature using `PlotDigitizer`.[139] We took the adsorption (as opposed to desorption) branch, though each MOF exhibited negligible-to-small adsorption/desorption hysteresis. Note, the water adsorption isotherms are step- or sigmoid-shaped, with transitions ranging from ∼15−35% relative humidity. The water adsorption capacities of the MOFs range from ∼0.35−0.48 kg H_2O/kg MOF. (Figures S1 and S2 compare the predicted water adsorption isotherms and step locations of all MOFs at the same temperature, 25 °C.) In summary, the water adsorption isotherms of these MOFs endow them with promise for achieving high water deliveries in an arid climate. More, the library of MOFs shows diversity in the water adsorption step locations, offering candidates for a range of different weather/climates.

3.1.1. Specialization in Climate/Weather Conditions. The diversity in the water adsorption isotherms among the candidate MOFs suggest specialization for particular capture and release conditions. For example, the step-transitions in the water adsorption isotherms of MIL-160 and MOF-303 occur at a lower relative humidity; meanwhile, the step-transitions of CAU-23 and Al-Fum occur at a higher relative humidity. Consequently, (1) on a warm and/or dry night, MIL-160 and MOF-303 are more suitable than CAU-23 and Al-Fum because they will capture much more water from the air; (2) on a cold and/or humid day, CAU-23 and Al-Fum are more suitable because they will still desorb their water obtained during the night, while MIL-160 and MOF-303 will hold onto their adsorbed water. This foreshadows that comprising a passive AWH adsorbent bed with *both* e.g., MOF-303 and CAU-23 could be advantageous over a time frame with highly variable humidity: on the dry nights, CAU-23 fails to capture water, but MOF-303 still does; on the humid days, MOF-303 fails to release its water, but CAU-23 delivers.

3.2. Case 1: Designing an Adsorbent Bed for AWH in the Chihuahuan Desert over the First 10 Days of June

For our first case study, suppose our passive AWH mission will take place in the Chihuahuan Desert of the United States, over the first 10 days of June, and our minimum daily demand for water is 2 kg/day. (We study a design for only a ten-day period (a) for parsimony, to lend an interpretable solution for gaining insights, and (b) to reflect the typical [only]-ten day weather forecast.)

3.2.1. Water Capture and Release Conditions. Figure 4 displays historical weather time series data in the Chihuahuan

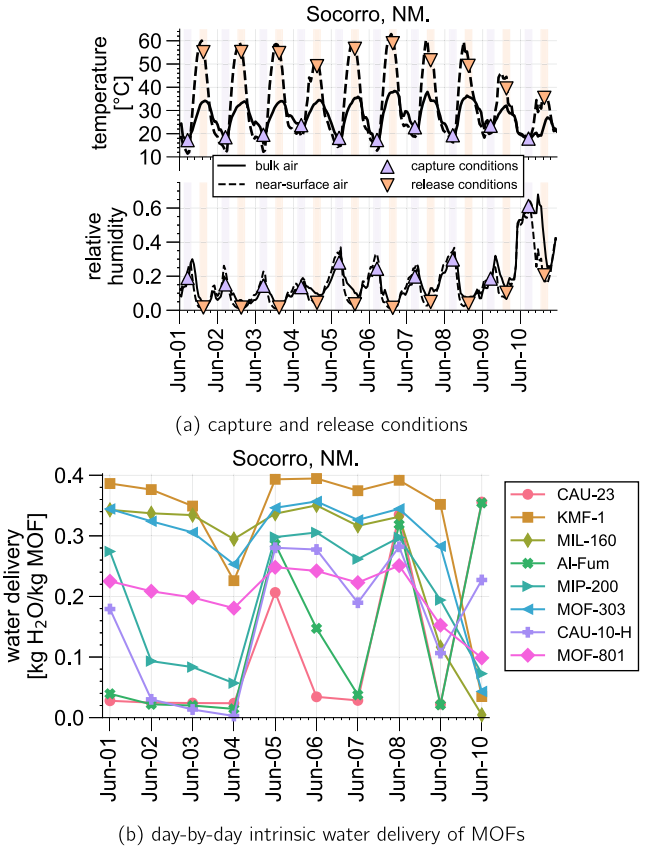

Figure 4. Predicted weather conditions and intrinsic water deliveries by the MOFs in the Chihuahuan Desert over the first 10 days of June. (a) Historical (2024; source:[99,100]) weather time series data and daily water capture and release conditions extracted from this data. (b) The predicted intrinsic water delivery by each MOF on each day.

desert and the predicted water capture and water release conditions on each day of the passive AWH mission. To predict the capture and release conditions on each day, we rely on historical (2024) weather data from a climate monitoring station[99,100] in Socorro, New Mexico. (See Section S1.1). Instruments at this station measure the hourly averaged temperature and relative humidity of the [bulk] air as well as the temperature of the surface of the land [exposed to natural sunlight]. We take the water capture conditions as the average temperature and relative humidity of the bulk air during the nighttime from 1 AM to 5 AM. For desorption conditions, we assume exposing the MOF bed to natural sunlight brings the MOF to the same temperature as the surface of the soil, which is higher than the bulk air temperature owing to solar irradiance. So, we take the release conditions as (i) for the

https://doi.org/10.1021/acsengineeringau.5c00051
ACS Eng. Au 2025, 5, 707−725

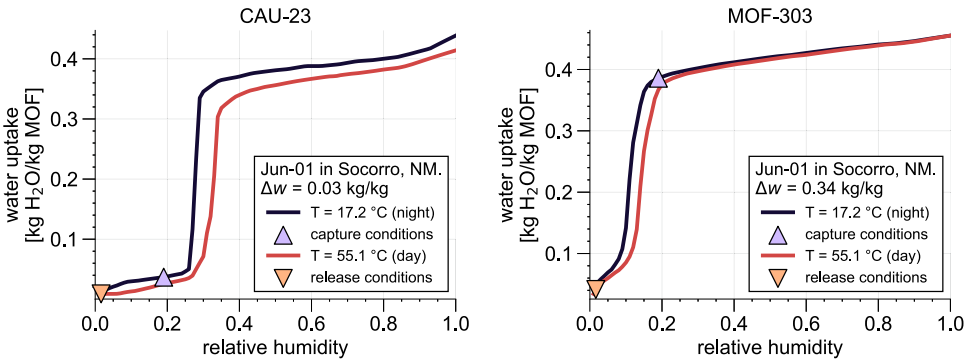

(a) day 1 (dry night): CAU-23 fails; MOF-303 delivers

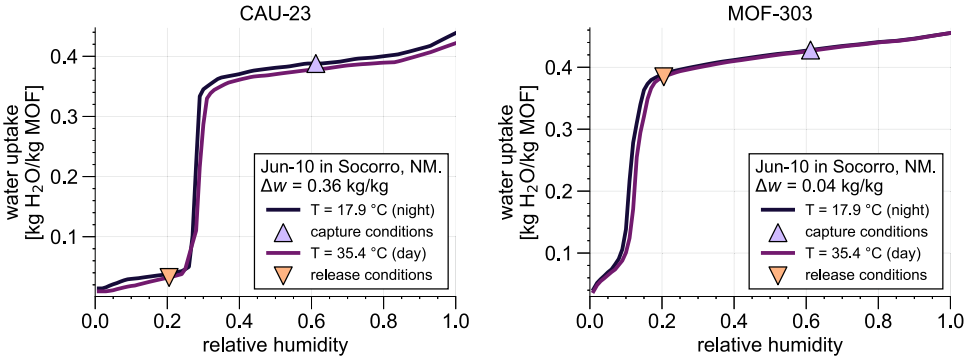

(b) day 10 (humid day): MOF-303 fails; CAU-23 delivers

Figure 5. Illustrating two mechanisms by which a MOF can fail to deliver water and specialization of MOFs to weather conditions. We compare the water deliveries of CAU-23 and MOF-303 on (a) day 1 and (b) day 10 of the AWH mission in the Chihuahuan Desert. Each panel shows the predicted water adsorption isotherms in the MOF at the capture and release temperature. The water delivery by the MOF is the water uptake at the nighttime, capture conditions minus the water uptake at the daytime, release conditions—both marked on the plot.

temperature, the average land surface temperature during the daytime from 1 to 5 PM and (ii) for the relative humidity, equivalent to the average water content of the daytime bulk air from 1 to 5 PM (*not* the relative humidity of the bulk daytime air, as the hotter air in the harvester exposed to sunlight can hold more moisture; see Section S1.2).

3.2.2. Daily Intrinsic Water Deliveries of the MOFs. Next, we predict the intrinsic water delivery [kg H_2O/kg MOF] by each candidate MOF on each day of the mission. Each water delivery follows from the predicted water adsorption at a capture condition minus the predicted water retained at the following release condition (see eq 1). For our implementation of a mathematical model for the equilibrium water adsorption $w^{(n)}(T, \phi)$ in each MOF $n \in [N]$ as a function of temperature T and relative humidity ϕ, we thermodynamically interpolate and -extrapolate the experimentally measured, equilibrium water adsorption isotherms in the MOFs (some shown in Figure 3b) using the Polanyi adsorption theory.[88] Particularly, we use a pseudo-Polanyi adsorption model for each MOF, where we interpolate [with respect to temperature] predictions of multiple Polanyi adsorption models obtained from multiple (if available) water adsorption isotherms. (See Sec. S1.3 for details; Figure S3 for all water adsorption data and characteristic curves along with predictions using Polanyi theory; Figure S4 as an example; and Figure S5 for alternative Dubinin-Astakhov and dual site Langmuir Freundlich models.)

Figure 4b shows the predicted intrinsic water deliveries by the MOFs on each day of the AWH mission. Owing to day-to-day variability in the capture and release conditions and differing water adsorption isotherms among the MOF structures: day-by-day, both the (1) intrinsic water delivery by a given MOF and (2) ranking of MOFs according to intrinsic water delivery, differ. KMF-1 exhibits the highest water delivery on 8/10 days of the mission as well as the highest average water delivery over the mission. But, KMF-1 shows a very poor water delivery on day 10 and only the third-highest delivery on day 4. MOF-801 exhibits the highest worst-case water delivery. Also quite satisfactory are MOF-303 and MIL-160. MOF-303 offers the 2nd-highest average water delivery and the 2nd-3rd highest water delivery on days 1−9. MIL-160 offers the third-highest average water delivery and the highest water delivery on day 4. Meanwhile, on day 10, Al-Fum and CAU-23 offer the highest water delivery. However, on days 1−4, 7, and 9, Al-Fum and CAU-23 exhibit very low water deliveries. Clearly, optimization of the composition of the MOF bed for this mission is an interesting, nontrivial, and challenging problem.

3.2.3. Illustrating Water Delivery Failure Modes and Specialization of MOFs to Particular Weather Conditions. Visualizing the water deliveries of CAU-23 and MOF-303 on day 1 and day 10 in Figure 5 illustrates two mechanisms by which MOFs can fail to deliver water and shows specialization of each MOF to particular weather conditions. First, day 1, whose nighttime is relatively dry (19% RH). Consequently, CAU-23, whose water adsorption step occurs at a high relative humidity, fails to adsorb significant water. Meanwhile, MOF-303, whose water adsorption step

https://doi.org/10.1021/acsengineeringau.5c00051
ACS Eng. Au 2025, 5, 707−725

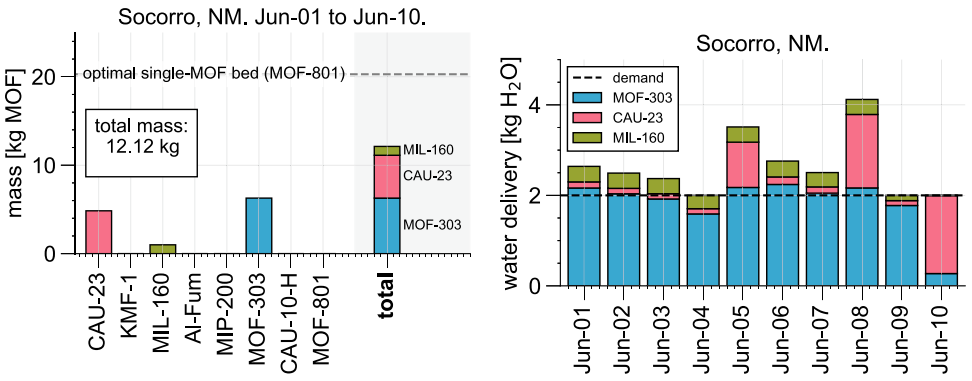

(a) optimal MOF bed make-up (b) daily water delivery by optimal bed

Figure 6. Optimal design of the composition of the mixed-MOF adsorbent bed for AWH in the Chihuahuan Desert over the first 10 days of June. (a) Optimal composition of the MOF bed. (b) Daily water delivery by the optimal MOF bed, broken down by MOF.

occurs at a low relative humidity, successfully captures water at night. Second, day 10, whose daytime is relatively humid (41% ambient RH) and cold (35.4 °C soil surface temperature). Now, the high-humidity water adsorption step of CAU-23 is advantageous. CAU-23 still desorbs its water during the day, while MOF-303 holds onto its water and thus fails to deliver much water. (Both CAU-23 and MOF-303 adsorb significant water the preceding night.) We make two conclusions. First, two mechanisms by which a MOF can fail to deliver water are (1) failing to adsorb water at night (like CAU-23 on day 1) and (2) failing to release its adsorbed water during the day (like MOF-303 on day 10). Second, loosely, MOF-303 specializes in capturing water on dry nights (like day 1), while CAU-23 specializes in delivering water on humid days (like day 10). (Note, day 4 shows an especially dry and warm night. Then, MOF-303 still performs well, but MIL-160 captures the most water at night. (See Figure S7.)

3.2.4. Optimal Composition of the Adsorbent Bed. Finally, we use the predicted intrinsic daily water delivery by the MOFs in Figure 4b to build the linear program in eq 4 that expresses our design principle for the composition of the MOF bed for the AWH mission. Specifically, we adjust the mass of each MOF making up the adsorbent bed to minimize the total mass of the bed under the constraints that at least 2 kg water is delivered on each day. Numerically solving the linear program gives the optimal composition of the MOF bed as the ternary mixture in Figure 6a: 52% MOF-303, 40% CAU-23, and 8% MIL-160 by weight, with a total mass of 12.12 kg for delivering at least 2 kg H_2O daily. As a baseline, restricting the bed to be composed of a single MOF leads to picking MOF-801 with the highest worst-case water delivery, requiring 20.3 kg of MOF-801 for delivering at least 2 kg H_2O daily.

Remarkably: First, the optimal mixed-MOF adsorbent bed is significantly (≈40%) lighter than the counterpart optimal single-MOF adsorbent bed, composed of MOF-801—which is not involved in the optimal mixture! (See Figure S6). Thus, entertaining the idea of adopting mixtures of MOFs for passive AWH, instead of restricting ourselves to a single MOF, can be fruitful. Second, the optimal adsorbent bed does not contain KMF-1, despite that KMF-1 exhibits (a) the highest average intrinsic water delivery and (b) the highest intrinsic water delivery on 8/10 days of the mission (see Figure 4b). This decision owes to KMF-1's poor water delivery on the fourth and 10th day. Thus, the MOF with the best *average* water delivery is not necessarily a good choice for comprising the adsorbent bed, as its variance [below the mean] in water delivery could be a detriment to robustness. Our linear program specifies a minimal-mass adsorbent bed composition that *consistently* meets the 2 kg H_2O daily water demand, rather than maximizing the total water delivered over the mission and accepting days where inadequate water is delivered (which would instead favor a pure KMF-1 bed).

3.2.5. Daily Water Delivery by the Mixed-MOF Adsorbent Bed. Figure 6b displays the [extrinsic] daily water delivery by the optimized mixed-MOF adsorbent bed, broken down by MOF. We make two remarks. First, the MOF-303 component of the bed provides the majority of the water on the first 9 days of the mission, whereas the CAU-23 component provides the majority (86%) of the water on day 10. Figure 5b explains why MOF-303 fails on the exceptionally humid day 10 while CAU-23 delivers: MOF-303 fails to desorb its water during the day. Second, the minimum daily drinking water demand is exactly met on days four, nine, and ten of the mission (i.e., the constraint is active). On the other days, more water is delivered than demanded (i.e., the constraint is inactive, and we have slack water). Solely the days corresponding with an active constraint present water capture and/or release conditions that restrict the adsorbent bed from being any lighter.

3.2.6. Robustness. By construction, our optimization problem in eq 4 specifies a design of the composition of the adsorbent bed that endows it with a water delivery *robust* to day-to-day variability in weather; i.e., we design the adsorbent bed to meet daily water demands in spite of fluctuations in humidity, temperature, and solar flux. The optimal solution is to compose the adsorbent bed with a ternary mixture of MOFs, namely 52% MOF-303, 40% CAU-23, and 8% MIL-160. First, carrying both CAU-23 and MOF-303/MIL-160 allowed for specialization of MOFs to delivering water on humid days and dry nights, respectively. When CAU-23 fails, MOF-303 delivers; and vice versa. Second, KMF-1 was excluded from the optimal bed despite exhibiting (1) the highest intrinsic water delivery among the MOFs for 8/10 days and (2) the highest average intrinsic water delivery over the time frame. A KMF-1-only bed of the same mass as our optimal mixed-MOF bed would have delivered more water *summed* over the time frame. But, on the 10th day, KMF-1 would have failed to deliver adequate water, due to exceptionally high humidity during the daytime. More, KMF-1 performs quite poorly on day 4 (see Figure S8); i.e., the daily

https://doi.org/10.1021/acsengineeringau.5c00051
ACS Eng. Au 2025, 5, 707−725

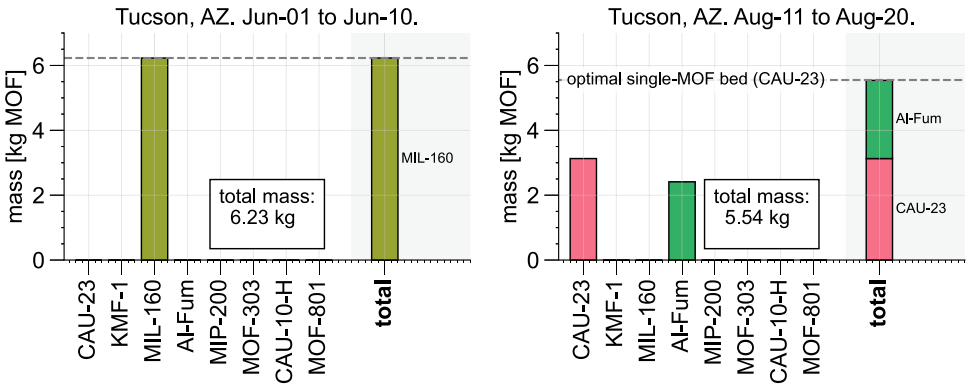

(a) optimal MOF bed composition, June (b) optimal MOF bed composition, August

Figure 7. Optimal design of the composition of a mixed-MOF adsorbent bed for passive AWH in the Sonoran Desert (a) in early June and (b) in middle August.

water delivery of a KMF-1 bed is not robust to variance in weather conditions, unlike our design in Figure 6a. Third, we rationalize the inclusion of MIL-160 because it exhibits the highest intrinsic water delivery on day 4, where the constraint is active.

3.3. Case 2: Designing an Adsorbent Bed for AWH in the Sonoran Desert

Next, we optimize the composition of a mixed-MOF adsorbent bed for passive AWH in a different region—the Sonoran Desert. Again, we impose a minimum daily water delivery of 2 kg. To obtain daily water capture and release conditions, we use historical (2024) time series data of the air temperature and humidity and land surface temperature in Tucson, Arizona, a city located within the Sonoran Desert.

3.3.1. AWH in the Sonoran Desert in Early-June. Figure 7a shows the optimal composition of the adsorbent bed for the first 10 days of June in the Sonoran Desert. Despite being for the same time frame as our design for the Chihuahuan Desert in Figure 6a, the design for the Sonoran Desert differs in two ways. First, the required mass of the adsorbent bed for the Sonoran Desert is approximately half that required for the Chihuahuan Desert. Second, the optimal makeup of the adsorbent bed differs—being solely MIL-160 for the Sonoran Desert. A mixture is not optimal. Explaining these results, (1) the capture and release conditions consistently fall above and below, respectively, the location of the step in water adsorption exhibited by MIL-160 and, consequently, (2) MIL-160 consistently exhibits the first-3rd highest intrinsic water delivery on each day of the time frame; the highest worst-case intrinsic water delivery; and the highest water delivery on the particularly challenging day 2 with the only active water delivery constraint (see Figure S9). This contrasts with the case study in the Chihuahuan Desert, where the particularly challenging day 10 presents a high daytime humidity above the water adsorption step for the MOFs that deliver plenty of water on days 1−9, necessitating a heavier adsorbent bed to meet demand on day 10 (absent day 10, the June 1−9 Chihuahuan Desert mission would require only 7.7 kg MOF).

3.3.2. AWH in the Sonoran Desert in Mid-August. Next, we find the optimal composition of the adsorbent bed for passive AWH in the Sonoran Desert in a different time frame—the middle of August. Interestingly, the optimal composition over this time frame, shown in Figure 7b, differs dramatically from the optimal composition in June, despite being for the same region. For mid-August, the optimal adsorbent bed is a binary mixture of 56% CAU-23 and 44% Al-Fum. The optimal bed for mid-August is c.a. 10% lighter than for early-June. Both Al-Fum and CAU-23 consistently provide a similarly high intrinsic water delivery on each day and retain performance on the particularly challenging day 8 (see Figure S10). As another interesting finding, the adoption of a binary mixture of MOFs does not confer a significant advantage for achieving a lighter adsorbent bed: the optimal mixed-MOF adsorbent bed is only 0.2% lighter than the optimal single-MOF (CAU-23) bed. This owes to the high similarity of the water adsorption isotherms of CAU-23 and Al-Fum.

3.4. Conclusions from Comparing Case Studies

Comparing the optimal designs in Figures 6a (Chihuahuan Desert; early June), 7a (Sonoran Desert; early June), and 7b (Sonoran Desert; middle August) leads us to several conclusions.

3.4.1. Importance of a Bespoke Design. The difference in optimal design of the composition of the adsorbent bed: (1) for the Chihuahuan Desert vs Sonoran Desert, both in early-June, highlights the importance of tailoring the composition of an adsorbent bed for passive AWH to the geographic region; (2) in early-June vs mid-August, both for the Sonoran Desert, highlight the importance of tailoring the composition of an adsorbent bed for passive AWH to the time frame. In conclusion, we highlight the importance of a *bespoke* design of an adsorbent bed for passive AWH, where its composition is tailored to both the geographic region and the time frame (i.e., season) in that region. In other words, a "universal" [among regions and times] formulation for the composition of an adsorbent bed for passive AWH is likely to be suboptimal with respect to specific regions and time frames.

3.4.2. Benefits (or Lack Thereof) of Mixtures. First, comprising the adsorbent bed for passive AWH with a *mixture* of MOFs does not always confer a lighter adsorbent bed than restricting ourselves to single-MOF adsorbent beds. For early June in the Sonoran Desert, we found a single-MOF bed is optimal—not a mixture. Second, when a mixture is optimal, we may obtain anywhere from very significant (e.g., 40% in early June in the Chihuahuan Desert) to only marginal (e.g., only 0.2% in mid-August in the Sonoran Desert) reductions in the mass of a single-MOF bed counterpart.

https://doi.org/10.1021/acsengineeringau.5c00051
ACS Eng. Au 2025, 5, 707−725

3.5. Visualizing a Reduced Linear Program

To gain insights, we visualize in Figure 8 the geometry of a reduced linear program for the optimal composition of an

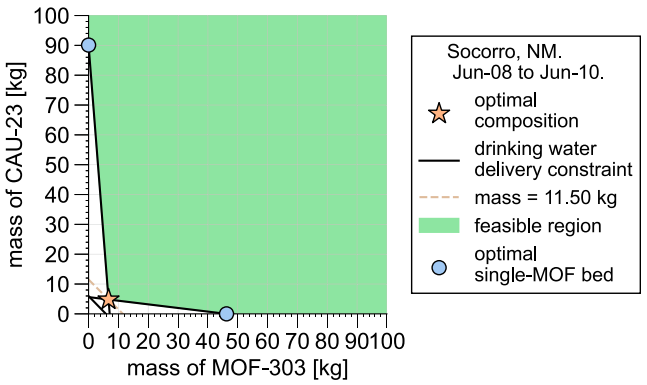

Figure 8. Visualizing a reduced linear program for optimizing the composition of a MOF bed for a passive AWH device under daily drinking water constraints.

adsorbent bed for passive AWH in the Chihuahuan Desert (a) over only 3 days (June 8−10) and (b) with only two MOF candidates, MOF-303 and CAU-23. Particularly, restricting to only two MOFs allows for visualization of the design space in the two-dimensional plane. Each solid, black line is a constraint line—one for each day—containing all compositions that deliver exactly q_d = 2 kg of water on that day. The feasible region of the design space, where the water delivery constraint is satisfied on each day, is shaded green. The feasible region is a convex polyhedron. Now, each line with slope negative one is a level set of the objective function, containing all compositions with a fixed mass. The optimal design, giving minimal mass, is marked with a star. Visually, we see the level set associated with the optimal design (a) cannot move further toward the origin without violating a constraint and (b) intersects a vertex of the feasible polyhedron corresponding with a mixed-MOF (as opposed to a single-MOF) design. Two of the constraints are active; one is inactive. For comparison, the two optimal (lightest) single-MOF beds that satisfy the constraints, marked with circles, are heavier than the optimal mixed-MOF bed.

With four or more candidate MOFs, we cannot visualize the high-dimensional design space, but a picture analogous to Figure 8 holds: (1) physically meaningful solutions lie in an orthant of the design space; (2) a minimum water delivery constraint on a given day enforces the solution to belong to a half-space (all points on or above a hyperplane); (3) the feasible region is a convex polyhedron formed by the intersection of these half-spaces; (4) at the optimal feasible design, the level set of the objective function, a hyperplane, will intersect a vertex (or, rarely, lie on a face) of this polyhedron. Intuitively, the simplex algorithm for numerically solving a linear program, essentially, walks along edges of the feasible polyhedron, from one vertex to a neighboring vertex with a better objective value, until no neighbor gives a better objective value.[125,140]

3.6. Sensitivity Analysis

The linear program in eq 4, specifying the optimal design of the adsorbent bed for a passive AWH mission, is based on uncertain data. First, the predicted intrinsic daily water deliveries by the candidate MOFs in $\mathbb{W}$ inherit uncertainty from both (a) the predicted capture and release conditions and (b) the predicted water adsorption in the MOFs at those conditions. Second, we may be unsure of the daily minimum water demands in $\mathbf{q}$. Third, the fraction of the water desorbed from the bed that we can condense and recover ξ is uncertain.

A sensitivity analysis of the linear program[141] investigates how the optimal design of the composition of the adsorbent bed responds to small changes in the predicted capture and release conditions, the water adsorption isotherms in the MOFs, the thermodynamic models, and/or the daily minimum water demands. Ideally, the design is quite insensitive to such changes. A brittle design that is highly unstable/sensitive to such changes may call for (1) the highest-fidelity (a) weather forecasting and (b) water adsorption data and modeling and/or (2) robust[142] or stochastic[143] optimization frameworks that explicitly treat uncertainty in the data. Sensitivities of the design to the water demands $\mathbf{q}$ indicate which days, if possible, we should supplement with another source of water to reduce water demand and allow for a lighter adsorbent bed.

To illustrate, we analyze the sensitivity of the optimal design of the adsorbent bed to perturbations in (i) the capture and release conditions; (ii) the water adsorption in the MOFs at the predicted capture and release conditions; and (iii) the daily water demand, both in the Chihuahuan Desert from June 1−10.

3.6.1. Sensitivity to Capture and Release Conditions.

To simulate scenarios with perturbed capture and release conditions, we add [i.i.d.] Gaussian errors to both the capture and release temperature and relative humidity (σ_T = 2 °C, σ_ϕ = 2%) on each day of the AWH mission. (In practice, the uncertainty in weather may grow with time.) We sample 100 such scenarios. For each scenario, we (i) predict the daily water delivery by the optimal design in Figure 6a and (ii) redesign the adsorbent bed for the perturbed capture and release conditions. Figure S10 analyzes the predicted water shortfalls of the current optimal design, if deployed under the perturbed capture and release conditions. The bed would not meet the water demand on one-to-three (usually two) days of the mission. The mean [over scenarios] worst-case [over days of the mission] water shortfall is 8%—not too severe. Regarding the ensemble of new designs tailored to these scenarios, Figure S11 shows the distribution of the total mass of the bed and the frequency that the different MOFs are involved, and Figure S12 displays a sample of 12 of the designs. The standard deviation of the mass of adsorbent needed over the scenarios is less than 5% of the mass of our current optimal design. Interestingly, most of the optimal designs in these perturbed scenarios contain a mixture of CAU-23 (also appearing in the design in Figure 6a) and KMF-1 (replacing MOF-303 in the design in Figure 6a).

3.6.2. Sensitivity to Water Adsorption in the MOFs.

We redesign the bed for eight scenarios where the predicted water delivery of one of the: (1) three MOFs composing the optimal adsorbent bed (MOF-303, CAU-23, MIL-160) is reduced by x% on each day and (2) five MOFs not contained in the optimal bed is increased by x%. The set of MOFs comprising the optimal bed is stable up to x = 3.3% changes in predicted water delivery. Increasing water delivery of Al-Fum or decreasing water delivery of CAU-23 by 5% leads to swapping CAU-23 for Al-Fum, with a < 2% change in the mass of the adsorbent bed. (Notably, the water adsorption steps for CAU-23 and Al-Fum occur at a similar relative humidity, giving a degree of exchangeability.) With a 7% reduction in MOF-303's water delivery, we swap MOF-303 for KMF-1, for

https://doi.org/10.1021/acsengineeringau.5c00051
ACS Eng. Au 2025, 5, 707−725

a 3.5% increase in the mass of the adsorbent bed. (Notably, the water adsorption steps for MOF-303 and KMF-1 occur at a similar relative humidity, giving a degree of exchangeability.)

3.6.3. Sensitivity to Daily Water Demand. Finally, we display the rate of change of the optimal mass of the bed with respect to small changes in the minimal daily water delivery on each day (i.e., shadow prices[141]) in Figure S13. The minimal mass of the adsorbent bed decreases when water demand is decreased (by a small amount) only on the 3 days when the water delivered exactly matches the minimal demand (i.e., when the constraint is active and there is no slack) and is most sensitive to changes in demand on the fourth and 10th day of the mission (c.a. three kg extra MOF required per kg extra H_2O demanded). Note, (1) we do not know on which days we exactly meet the minimal water demand until we solve the optimization problem and (2) shadow prices are invalid for sufficiently large changes in minimal water demand that alter which constraints are active.

4. CONCLUSION

We outlined and demonstrated a method to optimize the composition of a bespoke mixed-MOF adsorbent bed for robust passive AWH. Bespoke means the composition and total mass of the adsorbent bed is tailored to the weather/climate in a particular region and time frame. Robust means, despite variability in the weather (i.e., the capture and release conditions), the water delivery by the adsorbent bed meets or exceeds a daily water demand *on every day* of the time frame. Given a set of candidate MOFs, we framed a linear program that decides the mass of each MOF to constitute the adsorbent bed to minimize its total mass under hard constraints on the [predicted] water delivery on each day. Both [forecasted or historical] weather data in the region and water adsorption data in the candidate MOFs inform the linear program. We conclude that (1) optimized mixed-MOF adsorbent beds can be, but are not always, significantly lighter than optimized single-MOF adsorbent beds; (2) imposing a minimum water delivery on each day as a constraint enables the adsorbent bed to robustly [i.e., every day] meet water demands despite variability in weather; (3) both the composition and total mass of the optimal adsorbent bed differ by region, time frame, and daily water demands. Broadly, our work (1) is a starting point for the optimal design of bespoke mixed-MOF adsorbent beds for robust passive AWH and (2) puts forward the idea to adopt mixtures of MOFs for water harvesting, where each MOF specializes in delivering water under different categories of capture and release conditions. The future work we propose below can improve the fidelity of the design of adsorbent bed. Meanwhile, our sensitivity analysis showed how the optimal design responds to perturbations in the predicted capture and release conditions, the water adsorption data in the MOFs, and the daily minimum water demands.

Though we focused on adsorbent beds composed of MOFs, our design workflow and conclusions also pertain to other categories of porous materials for passive AWH, such as COFs.[57,58,144,145] As reticular nanoporous materials, COFs are also quite tunable in pore size, shape, and surface chemistry. Advantageously for AWH, COFs tend to be more stable than MOFs and lack metals that can leach into the water.[57]

5. DISCUSSION

5.1. Mixtures of MOFs

5.1.1. Realization. An adsorbent bed composed of multiple MOF structures could be realized in three ways. First, the powders of the distinct MOF structures, synthesized independently, could be physically mixed together. Second, mixed-MOF phases[86] could be synthesized in one batch, although normally this would result in limited control of the final phases and composition of the mixture. Third, each distinct MOF powder could be held in separate compartments of the AWH device. This method, a *portfolio* of MOFs, requires a more complicated AWH device but offers advantages of allowing facile (1) adjustment of the amount of each MOF comprising the bed and (2) nonsynchronous, targeted replacement of MOF constituents, as the least (most) stable MOF will need to be replaced most (least) frequently.

5.1.2. Mechanism to Fine-Tune Water Adsorption. Allowing the adsorbent bed to be composed of a mixture or portfolio of MOFs, as opposed to restricting ourselves to a single-MOF bed, simply grants us greater flexibility for adjusting the water adsorption of the bed as a function of temperature and relative humidity for optimal, robust passive AWH. Perhaps, multivariate MOFs and/or MOFs with multiple types of pores[146] for AWH could similarly grant such flexibility.[147,148]

5.2. Approximations, Caveats, and Limitations

Our model of the adsorbent bed for passive AWH makes several approximations. First, we neglect water adsorption−desorption hysteresis that some MOFs exhibit. Second, by assuming thermodynamic equilibrium, we neglect water and heat transfer limitations in the MOF during both the capture and release process.[149,150] Third, we neglect possible losses of water adsorption capacity in the MOFs over multiple capture-and-release cycles due to instability of the MOF structure.[44,70,73] Fourth, we neglect competitive (with water) adsorption of other gaseous components of the air, such as carbon dioxide. Interestingly, the concurrent capture of water and carbon dioxide from air has been proposed.[151,152] Fifth, on top of all of these approximations, we assume Polanyi adsorption theory can extrapolate an experimentally measured water adsorption isotherm in a MOF to other temperatures. Ideally, we would possess experimentally measured water adsorption data in the candidate MOFs that densely covers the pertinent temperature−humidity space. Sixth, we assume all of the water desorbed from the MOF can be condensed and collected (ξ = 1). Seventh, we [inevitably] rely on weather predictions (whether based on historical data or a numerical weather forecasting model[153]) in the region and time frame—which are subject to uncertainty. Eighth, we use the land surface temperature as a proxy for the MOF temperature under exposure to natural sunlight.

5.2.1. Comparison with a Field Study. A field- and laboratory-study[75] of passive AWH with MOF-801G found 40%−80% water delivery inefficiencies largely due to (1) heat and water transfer limitations in the MOF bed, which reduce both capture and release of water, and (2) incomplete condensation and collection of the water desorbed from the MOF. In Section S6 and Figure S14, we roughly compare the mass of MOF-801-G needed to deliver the 55 g of water collected in a passive AWH field study in Arizona during Oct. 2017 with our idealized calculation of the mass of MOF-801-G needed. We find 2.1 times the predicted weight of MOF-801-G

https://doi.org/10.1021/acsengineeringau.5c00051
ACS Eng. Au 2025, 5, 707−725

was needed in the field study. Perhaps, this suggests to set ξ in eq 4 to be around 1/2.

5.3. Extensions and Future Work

5.3.1. On Predicting the Water Delivery by the MOFs. Future work could improve the fidelity of the predicted water deliveries by the MOFs by accounting for the neglected physical phenomena of (a) heat and water transfer limitations; (b) coadsorption of species other than water; and/or (c) degradation of water adsorption in the MOF over time. This requires spatiotemporal models of the temperature of and density of adsorbed water in the adsorbent bed and MOF granules,[37] complex thermodynamic models of multicomponent gas adsorption in the MOFs, and temporal models of the decay of water adsorption in the MOFs over multiple adsorption−desorption cycles. These significant modeling undertakings would require (1) additional experimental data characterizing other properties of the MOFs (e.g., diffusion coefficient of water, water transfer coefficient, thermal conductivity, specific heat capacity, heat of adsorption of water, carbon dioxide adsorption) and (2) specifying or jointly optimizing the geometry of the adsorbent bed as well. The payoff in fidelity is likely MOF- and device-dependent.

Regarding capture and release conditions: For the capture conditions, we could account for passive radiative cooling of the device to the night sky to increase water adsorption.[32,35,154] For the release conditions, we might better-estimate the temperature of the MOF under sun exposure with knowledge of the solar flux and the MOFs' solar reflectances and infrared emissivities.[101] More, higher temperatures could be reached to desorb more water via employing a solar concentrator[155] or MOFs with high photothermal conversion.[44] Also, we might consider variation in the temperature and relative humidity over the few-hour capture and release process. Finally, an intriguing possibility to enhance water delivery may be via MOFs with moieties that undergo structural transformations upon exposure to sunlight to further drive out water and, perhaps, still release the water on a cold and humid day.[156,157]

5.3.2. On the Optimization Problem. Our optimization problem specifying the optimal composition of the adsorbent bed could be modified to handle different situations or encapsulate different design principles. First, we can allow water delivered in excess of demand (slack) on a given day to be saved and used later to satisfy the demand on future days. Second, we can estimate the economic cost c_n [$/kg MOF] of each MOF, then minimize the cost of the adsorbent bed, $\sum_{n=1}^{N} c_n m_n$, instead of its mass. Accounting for economies of scale for MOF production may render this a nonlinear program. Third, we could maximize the minimum daily water delivery over the time frame under a bed size constraint. Fourth, we could constrain or penalize the complexity of the bed design, measured by the number of distinct MOFs composing the adsorbent bed. Sixth, we could introduce constraints on the amount of a certain MOF comprising the adsorbent bed due to supply or production constraints. Seventh, we can allow for soft constraints and penalize constraint violations with slack variables in the objective function. Eighth, we can model uncertainty in the capture and release conditions with a probability distribution, then design the composition of the MOF bed by optimizing a risk metric[158] regarding its water delivery—formulating a stochastic program.[143] Alternatively, a robust optimization formulation would aim to satisfy the minimum daily water delivery demands under an uncertainty set of predicted intrinsic water deliveries by the MOFs.[142,159] Finally, we could instead minimize or place a constraint on the volume of the adsorbent bed. Then, we would also need to know the density of the MOF powder, if/how the powder is formed into e.g., pellets,[160] and how the powders or pellets of different MOFs pack together when mixed.

5.3.3. Coupling with Ongoing Research Efforts. Our work may be coupled with ongoing research directions for the design of new MOF structures with targeted water adsorption properties for AWH.[161] First, molecular simulations and machine learning models can rapidly predict water adsorption in thousands of hypothetical MOF crystal structure models.[71,119−124] Our framework in Figure 2 can be applied with simulated water adsorption data to screen a large database of hypothetical MOFs for promising candidates for passive AWH in a particular region. Second, our work links (a) water adsorption in an adsorbent bed as a function of temperature and humidity and (b) weather in a particular region and time frame, with passive AWH performance in that region and time frame—bypassing the precise structure of the MOF. Two other research efforts can inform the design of new MOF structures that afford the optimal water adsorption properties: (1) elucidating water adsorption mechanisms via both spectroscopy and molecular models[162−167] and (2) recognizing relationships between the structure and chemistry of MOFs and their water adsorption properties.[70−72] Third, predicting water stability of MOFs via machine learning or mechanistic insights[168−170] can provide more viable MOF candidates for AWH. Finally, broadly, our work may lead others to spot linear programs that naturally arise in the applied chemical sciences[171]—e.g., problems of blending products of crude oil refining[172] or allocating different categories of scrap steel to recycling processes that produce new categories of steel.[173]

5.3.4. Pursuit of MOF Mixtures for Other Gas Adsorption Tasks. Beyond AWH, many adsorption-based processes must cope with variance in the conditions (temperature, pressure, and composition) of the input gas over time and/or space. For example, the concentration of CO_2 in the air close to the ground varies significantly over the day owing to plants consuming CO_2 during during photosynthesis (at daytime) and releasing CO_2 during respiration (at nighttime).[174] And, the average humidity and temperature varies from region-to-region. Consequently, similarly, the design of an adsorbent bed and its operating conditions for direct-air CO_2 capture should be bespoke to a region and give robust performance against variance in the CO_2 concentration.[174−176]

■ ASSOCIATED CONTENT

Data Availability Statement

The raw data and Python code to reproduce all results and plots in this project are available at github.com/SimonEnsemble/water_harvesting.

Supporting Information

The Supporting Information is available free of charge at https://pubs.acs.org/doi/10.1021/acsengineeringau.5c00051.

(1) Detailed methods about the weather data, calculating the water release conditions, and applying Polanyi adsorption theory to model water adsorption in the MOFs; (2) exploration of alternative water adsorption models; (3) supplemental data visualizations pertaining to the AWH case study in the Chihuahuan

https://doi.org/10.1021/acsengineeringau.5c00051
ACS Eng. Au 2025, 5, 707−725

Desert; (4) supplemental data visualizations pertaining to the AWH case study in the Sonoran Desert; (5) data visualizations for the sensitivity analysis; and (6) comparison with a water harvesting field study (PDF)

AUTHOR INFORMATION

Corresponding Authors

Thijs J. H. Vlugt − *Engineering Thermodynamics, Process & Energy Department, Delft University of Technology, Delft 2628CB, The Netherlands*; Email: T.J.H.Vlugt@tudelft.nl

Ashlee J. Howarth − *Department of Chemistry and Biochemistry, Concordia University, Montréal, Quebec H4B 1R6, Canada*; orcid.org/0000-0002-9180-4084; Email: ashlee.howarth@concordia.ca

Cory M. Simon − *School of Chemical, Biological, and Environmental Engineering, Oregon State University, Corvallis, Oregon 97331, United States*; orcid.org/0000-0002-8181-9178; Email: cory.simon@oregonstate.edu

Authors

Charles Harriman − *School of Chemical, Biological, and Environmental Engineering, Oregon State University, Corvallis, Oregon 97331, United States*

Qia Ke − *School of Chemical, Biological, and Environmental Engineering, Oregon State University, Corvallis, Oregon 97331, United States*

Complete contact information is available at: https://pubs.acs.org/10.1021/acsengineeringau.5c00051

Notes

The authors declare no competing financial interest.

ACKNOWLEDGMENTS

C.H. was supported by the DeVaan Experiential Learning Fund under Oregon State University's Clean Water Initiative. Q.K. acknowledges Scialog grant #SA-AUT-2024-017b from Research Corporation for Science Advancement and Arnold and Mabel Beckman Foundation. A.J.H. acknowledges the Concordia University Research Chair Program. C.M.S. acknowledges the U.S. National Science Foundation Award #2421968. We thank the anonymous reviewers for their helpful comments that led to improvements in our paper.

REFERENCES

(1) Gleick, P. H.; Cooley, H. Freshwater scarcity. *Annu. Rev. Environ. Resour.* **2021**, *46* (1), 319−348.

(2) Postel, S. L.; Daily, G. C.; Ehrlich, P. R. Human appropriation of renewable fresh water. *Science* **1996**, *271* (5250), 785−788.

(3) Hoekstra, A. Y. Human appropriation of natural capital: A comparison of ecological footprint and water footprint analysis. *Ecol. Econ.* **2009**, *68* (7), 1963−1974.

(4) Mekonnen, M. M.; Hoekstra, A. Y. Four billion people facing severe water scarcity. *Sci. Adv.* **2016**, *2* (2), No. e1500323.

(5) Schweitzer, L.; Noblet, J. Water Contamination and Pollution. In *Green Chemistry*; Elsevier, 2018; pp 261−290.

(6) Vorosmarty, C. J.; Green, P.; Salisbury, J.; Lammers, R. B. Global water resources: vulnerability from climate change and population growth. *Science* **2000**, *289* (5477), 284−288.

(7) Schewe, J.; Heinke, J.; Gerten, D.; Haddeland, I.; Arnell, N. W.; Clark, D. B.; Dankers, R.; Eisner, S.; Fekete, B. M.; Colón-González, F. J.; Gosling, S. N.; Kim, H.; Liu, X.; Masaki, Y.; Portmann, F. T.; Satoh, Y.; Stacke, T.; Tang, Q.; Wada, Y.; Wisser, D.; Albrecht, T.; Frieler, K.; Piontek, F.; Warszawski, L.; Kabat, P. Multimodel assessment of water scarcity under climate change. *Proc. Natl. Acad. Sci. U.S.A.* **2014**, *111* (9), 3245−3250.

(8) Gleick, P. H. Water use. *Annu. Rev. Environ. Resour.* **2003**, *28* (1), 275−314.

(9) He, C.; Liu, Z.; Wu, J.; Pan, X.; Fang, Z.; Li, J.; Bryan, B. A. Future global urban water scarcity and potential solutions. *Nat. Commun.* **2021**, *12* (1), No. 4667.

(10) Larsen, T. A.; Hoffmann, S.; Lüthi, C.; Truffer, B.; Maurer, M. Emerging solutions to the water challenges of an urbanizing world. *Science* **2016**, *352* (6288), 928−933.

(11) Wada, Y.; Gleeson, T.; Esnault, L. Wedge approach to water stress. *Nat. Geosci.* **2014**, *7* (9), 615−617.

(12) Gude, V. G. Desalination and sustainability−an appraisal and current perspective. *Water Res.* **2016**, *89*, 87−106.

(13) Tundisi, J. G. Reservoirs: New challenges for ecosystem studies and environmental management. *Water Secur.* **2018**, *4-5*, 1−7.

(14) Liu, X.; Beysens, D.; Bourouina, T. Water harvesting from air: Current passive approaches and outlook. *ACS Mater. Lett.* **2022**, *4* (5), 1003−1024.

(15) Humphrey, J. H.; Brown, J.; Cumming, O.; Evans, B.; Howard, G.; Kulabako, R. N.; Lamontagne, J.; Pickering, A. J.; Wang, E. N. The potential for atmospheric water harvesting to accelerate household access to safe water. *Lancet Planetary Health* **2020**, *4* (3), e91−e92.

(16) Parker, A. R.; Lawrence, C. R. Water capture by a desert beetle. *Nature* **2001**, *414* (6859), 33−34.

(17) Roth-Nebelsick, A.; Ebner, M.; Miranda, T.; Gottschalk, V.; Voigt, D.; Gorb, S.; Stegmaier, T.; Sarsour, J.; Linke, M.; Konrad, W. Leaf surface structures enable the endemic Namib desert grass Stipagrostis sabulicola to irrigate itself with fog water. *J. R. Soc., Interface* **2012**, *9* (73), 1965−1974.

(18) Ju, J.; Bai, H.; Zheng, Y.; Zhao, T.; Fang, R.; Jiang, L. A multi-structural and multi-functional integrated fog collection system in cactus. *Nat. Commun.* **2012**, *3* (1), No. 1247.

(19) Pan, Z.; Pitt, W. G.; Zhang, Y.; Wu, N.; Tao, Y.; Truscott, T. T. The upside-down water collection system of Syntrichia caninervis. *Nat. Plants* **2016**, *2* (7), No. 16076.

(20) Gurera, D.; Bhushan, B. Passive water harvesting by desert plants and animals: lessons from nature. *Philos. Trans. R. Soc., A* **2020**, *378* (2167), No. 20190444.

(21) Zheng, Y.; Bai, H.; Huang, Z.; Tian, X.; Nie, F.-Q.; Zhao, Y.; Zhai, J.; Jiang, L. Directional water collection on wetted spider silk. *Nature* **2010**, *463* (7281), 640−643.

(22) Bhushan, B. Bioinspired water collection methods to supplement water supply. *Philos. Trans. R. Soc., A* **2019**, *377* (2150), No. 20190119.

(23) Ahrestani, Z.; Sadeghzadeh, S.; Emrooz, H. B. M. An overview of atmospheric water harvesting methods, the inevitable path of the future in water supply. *RSC Adv.* **2023**, *13* (15), 10273−10307.

(24) Tu, Y.; Wang, R.; Zhang, Y.; Wang, J. Progress and expectation of atmospheric water harvesting. *Joule* **2018**, *2* (8), 1452−1475.

(25) Tu, R.; Hwang, Y. Reviews of atmospheric water harvesting technologies. *Energy* **2020**, *201*, No. 117630.

(26) Lu, H.; Shi, W.; Guo, Y.; Guan, W.; Lei, C.; Yu, G. Materials engineering for atmospheric water harvesting: Progress and perspectives. *Adv. Mater.* **2022**, *34* (12), No. 2110079.

(27) Xiang, T.; Xie, S.; Chen, G.; Zhang, C.; Guo, Z. Recent advances in atmospheric water harvesting technology and its development. *Mater. Horiz.* **2025**, *12*, 1084−1105.

(28) Wang, B.; Zhou, X.; Guo, Z.; Liu, W. Recent advances in atmosphere water harvesting: Design principle, materials, devices, and applications. *Nano Today* **2021**, *40*, No. 101283.

(29) Park, K.-C.; Chhatre, S. S.; Srinivasan, S.; Cohen, R. E.; McKinley, G. H. Optimal design of permeable fiber network structures for fog harvesting. *Langmuir* **2013**, *29* (43), 13269−13277.

(30) Klemm, O.; Schemenauer, R. S.; Lummerich, A.; Cereceda, P.; Marzol, V.; Corell, D.; Heerden, J. V.; Reinhard, D.; Gherezghiher, T.; Olivier, J.; Osses, P.; Sarsour, J.; Frost, E.; Estrela, M. J.; Valiente, J. A.; Fessehaye, G. M. Fog as a fresh-water resource: overview and perspectives. *Ambio* **2012**, *41*, 221−234.

(31) Kennedy, B. S.; Boreyko, J. B. Bio-inspired fog harvesting meshes: a review. *Adv. Funct. Mater.* **2024**, *34* (35), No. 2306162.
(32) Khalil, B.; Adamowski, J.; Shabbir, A.; Jang, C.; Rojas, M.; Reilly, K.; Ozga-Zielinski, B. A review: dew water collection from radiative passive collectors to recent developments of active collectors. *Sustainable Water Resour. Manage.* **2016**, *2*, 71−86.
(33) Gido, B.; Friedler, E.; Broday, D. M. Assessment of atmospheric moisture harvesting by direct cooling. *Atmos. Res.* **2016**, *182*, 156−162.
(34) Lee, A.; Moon, M.-W.; Lim, H.; Kim, W.-D.; Kim, H.-Y. Water harvest via dewing. *Langmuir* **2012**, *28* (27), 10183−10191.
(35) Kim, H.; Rao, S. R.; Kapustin, E. A.; Zhao, Lin.; Yang, S.; Yaghi, O. M.; Wang, E. N. Adsorption-based atmospheric water harvesting device for arid climates. *Nat. Commun.* **2018**, *9* (1), No. 1191.
(36) Jia, L.; Hu, Y.; Liu, Z.; Hao, H.; Xu, H.; Huang, W.; He, X. Porous materials MOFs and COFs: Energy-saving adsorbents for atmospheric water harvesting. *Mater. Today* **2024**, *78*, 92−111.
(37) LaPotin, A.; Kim, H.; Rao, S. R.; Wang, E. N. Adsorption-based atmospheric water harvesting: impact of material and component properties on system-level performance. *Acc. Chem. Res.* **2019**, *52* (6), 1588−1597.
(38) Wang, J. Y.; Wang, R. Z.; Wang, L. W.; Liu, J. Y. A high efficient semi-open system for fresh water production from atmosphere. *Energy* **2017**, *138*, 542−551.
(39) Zhou, X.; Lu, H.; Zhao, F.; Yu, G. Atmospheric water harvesting: A review of material and structural designs. *ACS Mater. Lett.* **2020**, *2* (7), 671−684.
(40) Li, R.; Wang, P. Sorbents, processes and applications beyond water production in sorption-based atmospheric water harvesting. *Nat. Water* **2023**, *1* (7), 573−586.
(41) Meng, Y.; Dang, Y.; Suib, S. L. Materials and devices for atmospheric water harvesting. *Cell Rep. Phys. Sci.* **2022**, *3*, No. 100976, DOI: 10.1016/j.xcrp.2022.100976.
(42) Entezari, A.; Esan, O. C.; Yan, X.; Wang, R.; An, L. Sorption-based atmospheric water harvesting: Materials, components, systems, and applications. *Adv. Mater.* **2023**, *35* (40), No. 2210957.
(43) Kalmutzki, M. J.; Diercks, C. S.; Yaghi, O. M. Metal−organic frameworks for water harvesting from air. *Adv. Mater.* **2018**, *30* (37), No. 1704304.
(44) Hu, Y.; Ye, Z.; Peng, X. Metal-organic frameworks for solar-driven atmosphere water harvesting. *Chem. Eng. J.* **2023**, *452*, No. 139656.
(45) Shi, W.; Guan, W.; Lei, C.; Yu, G. Sorbents for atmospheric water harvesting: from design principles to applications. *Angew. Chem.* **2022**, *134* (43), No. e202211267.
(46) Bai, S.; Yao, X.; Wong, M. Y.; Xu, Q.; Li, H.; Lin, K.; Zhou, Y.; Ho, T. C.; Pan, A.; Chen, J.; Zhu, Y.; Wang, S.; Tso, C. Y. Enhancement of water productivity and energy efficiency in sorption-based atmospheric water harvesting systems: From material, component to system level. *ACS Nano* **2024**, *18* (46), 31597−31631.
(47) Lei, C.; Guan, W.; Zhao, Y.; Yu, G. Chemistries and materials for atmospheric water harvesting. *Chem. Soc. Rev.* **2024**, *53* (14), 7328−7362.
(48) Feng, A.; Akther, N.; Duan, X.; Peng, S.; Onggowarsito, C.; Mao, S.; Fu, Q.; Kolev, S. D. Recent development of atmospheric water harvesting materials: a review. *ACS Mater. Au* **2022**, *2* (5), 576−595.
(49) Xu, W.; Yaghi, O. M. Metal−organic frameworks for water harvesting from air, anywhere, anytime. *ACS Cent. Sci.* **2020**, *6* (8), 1348−1354.
(50) Hanikel, N.; Prévot, M. S.; Yaghi, O. M. MOF water harvesters. *Nat. Nanotechnol.* **2020**, *15* (5), 348−355.
(51) Shan, H.; Li, C.; Chen, Z.; Ying, W.; Poredoš, P.; Ye, Z.; Pan, Q.; Wang, J.; Wang, R. Exceptional water production yield enabled by batch-processed portable water harvester in semi-arid climate. *Nat. Commun.* **2022**, *13* (1), No. 5406.
(52) LaPotin, A.; Zhong, Y.; Zhang, L.; Zhao, L.; Leroy, A.; Kim, H.; Rao, S. R.; Wang, E. N. Dual-stage atmospheric water harvesting device for scalable solar-driven water production. *Joule* **2021**, *5* (1), 166−182.
(53) Wang, J. Y.; Wang, R. Z.; Tu, Y. D.; Wang, L. W. Universal scalable sorption-based atmosphere water harvesting. *Energy* **2018**, *165*, 387−395.
(54) Deng, F.; Poredoš, P.; Yu, J.; Chen, Z.; Xiang, C.; Yang, X.; Wang, R. Ultra-high-yield solar-driven modular atmospheric water harvester with improved heat management. *Device* **2024**, *2*, No. 100441, DOI: 10.1016/j.device.2024.100441.
(55) Borne, I.; Cooper, A. I. Sorbent-based atmospheric water harvesting: engineering challenges from the process to molecular scale. *J. Mater. Chem. A* **2025**, *13*, 4838−4850.
(56) Lyu, T.; Han, Y.; Chen, Z.; Fan, X.; Tian, Ye. Hydrogels and hydrogel derivatives for atmospheric water harvesting. *Mater. Today Sustainability* **2024**, *25*, No. 100693.
(57) Nguyen, H. L. Covalent organic frameworks for atmospheric water harvesting. *Adv. Mater.* **2023**, *35* (17), No. 2300018.
(58) Wen, F.; Huang, N. Covalent organic frameworks for water harvesting from air. *ChemSusChem* **2024**, *17* (13), No. e202400049.
(59) Kim, H.; Yang, S.; Rao, S. R.; Narayanan, S.; Kapustin, E. A.; Furukawa, H.; Umans, A. S.; Yaghi, O. M.; Wang, E. N. Water harvesting from air with metal-organic frameworks powered by natural sunlight. *Science* **2017**, *356* (6336), 430−434.
(60) Furukawa, H.; Gándara, F.; Zhang, Y.-B.; Jiang, J.; Queen, W. L.; Hudson, M. R.; Yaghi, O. M. Water adsorption in porous metal−organic frameworks and related materials. *J. Am. Chem. Soc.* **2014**, *136* (11), 4369−4381.
(61) Song, W.; Zheng, Z.; Alawadhi, A. H.; Yaghi, O. M. MOF water harvester produces water from Death Valley desert air in ambient sunlight. *Nat. Water* **2023**, *1* (7), 626−634.
(62) Feng, Y.; Wang, R.; Ge, T. Full passive MOF water harvester in a real desert climate. *Device* **2023**, *1* (2), No. 100054.
(63) Zhang, B.; Zhu, Z.; Wang, X.; Liu, X.; Kapteijn, F. Water adsorption in MOFs: structures and applications. *Adv. Funct. Mater.* **2024**, *34* (43), No. 2304788.
(64) Howarth, A. J.; Quezada-Novoa, V.; Copeman, C.; Donnarumma, P. R. *Metal-Organic Frameworks for Clean Water Generation: from Purification to Harvesting* De Gruyter: Berlin, Boston, 2023; pp 301−338.
(65) Furukawa, H.; Cordova, K. E.; O'Keeffe, M.; Yaghi, O. M. The chemistry and applications of metal-organic frameworks. *Science* **2013**, *341*, No. 1230444, DOI: 10.1126/science.1230444.
(66) Liu, X.; Wang, X.; Kapteijn, F. Water and metal−organic frameworks: From interaction toward utilization. *Chem. Rev.* **2020**, *120* (16), 8303−8377.
(67) Song, Y.; Zeng, M.; Wang, X.; Shi, P.; Fei, M.; Zhu, J. Hierarchical engineering of sorption-based atmospheric water harvesters. *Adv. Mater.* **2024**, *36* (12), No. 2209134.
(68) Moghadam, P. Z.; Li, A.; Wiggin, S. B.; Tao, A.; Maloney, A. G. P.; Wood, P. A.; Ward, S. C.; Fairen-Jimenez, D. Development of a Cambridge Structural Database subset: a collection of metal−organic frameworks for past, present, and future. *Chem. Mater.* **2017**, *29* (7), 2618−2625.
(69) Zhao, G.; Brabson, L. M.; Chheda, S.; Huang, J.; Kim, H.; Liu, K.; Mochida, K.; Pham, T. D.; Prerna; Terrones, G. G.; Yoon, S.; Zoubritzky, L.; Coudert, F.-X.; Haranczyk, M.; Kulik, H. J.; Moosavi, S. M.; Sholl, D. S.; Siepmann, J. I.; Snurr, R. Q.; Chung, Y. G. CoRE MOF DB: A curated experimental metal-organic framework database with machine-learned properties for integrated material-process screening. *Matter* **2025**, *8* (6), No. 102140.
(70) Canivet, J.; Bonnefoy, J.; Daniel, C.; Legrand, A.; Coasne, B.; Farrusseng, D. Structure−property relationships of water adsorption in metal−organic frameworks. *New J. Chem.* **2014**, *38* (7), 3102−3111.
(71) Shih, S.-M.; Lin, L.-C. Water adsorption in metal−organic frameworks: Characteristics, mechanisms, and structure−property relationships. *J. Am. Chem. Soc.* **2025**, *147* (38), 34791−34803.
(72) Xu, M.; Liu, Z.; Huai, X.; Lou, L.; Guo, J. Screening of metal−organic frameworks for water adsorption heat transformation using

structure−property relationships. *RSC Adv.* **2020**, *10* (57), 34621−34631.
(73) Burtch, N. C.; Jasuja, H.; Walton, K. S. Water stability and adsorption in metal−organic frameworks. *Chem. Rev.* **2014**, *114* (20), 10575−10612.
(74) Rojas, S.; Horcajada, P. Metal−organic frameworks for the removal of emerging organic contaminants in water. *Chem. Rev.* **2020**, *120* (16), 8378−8415.
(75) Fathieh, F.; Kalmutzki, M. J.; Kapustin, E. A.; Waller, P. J.; Yang, J.; Yaghi, O. M. Practical water production from desert air. *Sci. Adv.* **2018**, *4* (6), No. eaat3198.
(76) Lassitter, T.; Hanikel, N.; Coyle, D. J.; Hossain, M. I.; Lipinski, B.; O'Brien, M.; Hall, D. B.; Hastings, J.; Borja, J.; O'Neil, T.; Neumann, S. E.; Moore, D. R.; Yaghi, O. M.; Glover, T. G. Mass transfer in atmospheric water harvesting systems. *Chem. Eng. Sci.* **2024**, *285*, No. 119430.
(77) Hanikel, N.; Prévot, M. S.; Fathieh, F.; Kapustin, E. A.; Lyu, H.; Wang, H.; Diercks, N. J.; Glover, T. G.; Yaghi, O. M. Rapid cycling and exceptional yield in a metal-organic framework water harvester. *ACS Cent. Sci.* **2019**, *5* (10), 1699−1706.
(78) Li, X.; El Fil, B.; Fil, B. E.; Li, B.; Graeber, G.; Li, A. C.; Li, A. C.; Zhong, Y.; Zhong, Y.; Alshrah, M.; Alshrah, M.; Wilson, C. T.; Wilson, C. T.; Lin, E. Design of a compact multicyclic high-performance atmospheric water harvester for arid environments. *ACS Energy Lett.* **2024**, *9* (7), 3391−3399.
(79) Kim, J.; Jamdade, S.; Yuan, Y.; Realff, M. J. Metal-organic frameworks for atmospheric water extraction: Kinetic analysis and stochastic programming under climate variability. *J. Cleaner Prod.* **2024**, *482*, No. 144187.
(80) Guo, S.; Zhang, Y.; Tan, S. C. Device design and optimization of sorption-based atmospheric water harvesters. *Device* **2023**, *1* (4), No. 100099.
(81) Kim, H.; Rao, S. R.; LaPotin, A.; Lee, S.; Wang, E. N. Thermodynamic analysis and optimization of adsorption-based atmospheric water harvesting. *Int. J. Heat Mass Transfer* **2020**, *161*, No. 120253.
(82) Gildernew, E.; Yang, S. Finite element modeling of atmospheric water extraction by way of highly porous adsorbents: A roadmap for solver construction with model factor sensitivity screening. *J. Chem. Inf. Model.* **2022**, *62* (17), 4149−4161.
(83) Wilson, C. T.; Cha, H.; Zhong, Y.; Li, A. C.; Lin, E.; Fil, B. E. Design considerations for next-generation sorbent-based atmospheric water-harvesting devices. *Device* **2023**, *1* (2), No. 100052.
(84) Feng, Y.; Wang, R.; Ge, T. Pathways to energy-efficient water production from the atmosphere. *Adv. Sci.* **2022**, *9* (36), No. 2204508.
(85) Ward, A.; Li, K.; Pini, R. Assessment of dual-adsorbent beds for CO_2 capture by equilibrium-based process design. *Sep. Purif. Technol.* **2023**, *319*, No. 123990.
(86) Schlüsener, C.; Jordan, D. N.; Xhinovci, M.; Ntep, T. J. M. M.; Schmitz, A.; Giesen, B.; Janiak, C. Probing the limits of linker substitution in aluminum mofs through water vapor sorption studies: mixed-mofs instead of mixed-linker CAU-23 and MIL-160 materials. *Dalton Trans.* **2020**, *49* (22), 7373−7383.
(87) Beck, A.; Guttmann-Beck, N. *A First Course in Linear Optimization*; SIAM, 2025.
(88) Polanyi, M. Section III.—theories of the adsorption of gases. a general survey and some additional remarks. *Trans. Faraday Soc.* **1932**, *28* (0), 316−333.
(89) Ma, C.; Li, J.; Wang, G.; Li, Z.; Su, W.; Zhou, Y. Microscopic kinetics of water adsorption in metal−organic frameworks. *Nano Lett.* **2025**, *25* (14), 5778−5783.
(90) Madden, D. G.; Scott, H. S.; Kumar, A.; Chen, K.-J.; Sanii, R.; Bajpai, A.; Lusi, M.; Curtin, T.; Perry, J. J.; Zaworotko, M. J. Flue-gas and direct-air capture of CO_2 by porous metal−organic materials. *Philos. Trans. R. Soc., A* **2017**, *375* (2084), No. 20160025.
(91) Mukherjee, S.; Sikdar, N.; O'Nolan, D.; Franz, D.M.; Gascón, V.; Kumar, A.; Kumar, N.; Scott, H. S.; Madden, D. G.; Kruger, P. E.; Space, B.; Zaworotko, M. J. Trace CO_2 capture by an ultra-microporous physisorbent with low water affinity. *Sci. Adv.* **2019**, *5* (11), No. eaax9171.
(92) Krishna, R.; van Baten, J. M. How reliable is the real adsorbed solution theory (RAST) for estimating ternary mixture equilibrium in microporous host materials? *Fluid Phase Equilib.* **2025**, *589*, No. 114260.
(93) Krishna, R.; van Baten, J. M. Non-idealities in adsorption thermodynamics for CO_2 capture from humid natural gas using CALF-20. *Sep. Purif. Technol.* **2025**, *355*, No. 129553.
(94) Krishna, R.; van Baten, J. M. Elucidating the failure of the ideal adsorbed solution theory for CO_2/H_2O mixture adsorption in CALF-20. *Sep. Purif. Technol.* **2025**, *352*, No. 128269.
(95) Krishna, R.; van Baten, J. M. Highlighting the technological consequences of thermodynamic non-idealities in mixture separations using microporous crystalline adsorbents. *Sep. Purif. Technol.* **2025**, *362*, No. 131757.
(96) Krishna, R.; van Baten, J. M. How reliable is the ideal adsorbed solution theory for the estimation of mixture separation selectivities in microporous crystalline adsorbents? *ACS Omega* **2021**, *6* (23), 15499−15513.
(97) Krishna, R. Evaluation of procedures for estimation of the isosteric heat of adsorption in microporous materials. *Chem. Eng. Sci.* **2015**, *123*, 191−196.
(98) Nicks, J.; Mudure, C.; James, J.; McDougall, A.; Hughes, W. O. H.; Spencer, J.; Düren, T.; Burrows, A. D. Particle size effects on vapour uptake and release dynamics in metal−organic frameworks. *Chem. Commun.* **2025**, *61* (41), 7490−7493.
(99) Diamond, H. J.; Karl, T. R.; Palecki, M. A.; Baker, C. B.; Bell, J. E.; Leeper, R. D.; Easterling, D. R.; Lawrimore, J. H.; Meyers, T. P.; Helfert, M. R.; Goodge, G.; Thorne, P. W. U.S. climate reference network after one decade of operations: Status and assessment. *Bull. Am. Meteorol. Soc.* **2013**, *94* (4), 485−498.
(100) Bell, J. E.; Palecki, M. A.; Baker, C. B.; Collins, W. G.; Lawrimore, J. H.; Leeper, R. D.; Hall, M. E.; Kochendorfer, J.; Meyers, T. P.; Wilson, T.; Diamond, H. J. U.S. climate reference network soil moisture and temperature observations. *J. Hydrometeorol.* **2013**, *14* (3), 977−988.
(101) Lam, D. V.; Dung, D. T.; Nguyen, U. N. T.; Kang, H. S.; Bae, B.-S.; Kim, H.-D.; Lim, M.; Kim, D.; Kim, J.-H.; Lee, S.-M. Metal-organic frameworks as a thermal emitter for high-performance passive radiative cooling. *Small Methods* **2025**, *9* (3), No. 2401141.
(102) AbdulHalim, R. G.; Bhatt, P. M.; Belmabkhout, Y.; Shkurenko, A.; Adil, K.; Barbour, L. J.; Eddaoudi, M. A fine-tuned metal−organic framework for autonomous indoor moisture control. *J. Am. Chem. Soc.* **2017**, *139* (31), 10715−10722.
(103) Kumar, A.; Madden, D. G.; Lusi, M.; Chen, K.-J.; Daniels, E. A.; Curtin, T.; Perry, J. J., IV; Zaworotko, M. J. Direct air capture of CO_2 by physisorbent materials. *Angew. Chem., Int. Ed.* **2015**, *54* (48), 14372−14377.
(104) Tan, K.; Zuluaga, S.; Gong, Q.; Gao, Y.; Nijem, N.; Li, J.; Thonhauser, T.; Chabal, Y. J. Competitive coadsorption of CO_2 with H_2O, NH_3, SO_2, NO, NO_2, N_2, O_2, and CH_4 in M-MOF-74 (M = Mg, Co, Ni): the role of hydrogen bonding. *Chem. Mater.* **2015**, *27* (6), 2203−2217.
(105) Kolle, J. M.; Fayaz, M.; Sayari, A. Understanding the effect of water on CO_2 adsorption. *Chem. Rev.* **2021**, *121* (13), 7280−7345.
(106) Findley, J. M.; Sholl, D. S. Computational screening of MOFs and zeolites for direct air capture of carbon dioxide under humid conditions. *J. Phys. Chem. C* **2021**, *125* (44), 24630−24639.
(107) Sriram, A.; Choi, S.; Yu, X.; Brabson, L. M.; Das, A.; Ulissi, Z.; Uyttendaele, M.; Medford, A. J.; Sholl, D. S. The Open DAC 2023 Dataset and challenges for sorbent discovery in direct air capture. *ACS Cent. Sci.* **2024**, *10* (5), 923−941.
(108) Carsch, K. M.; Huang, A. J.; Dods, M. N.; Parker, S. T.; Rohde, R. C.; Jiang, H. Z. H.; Yabuuchi, Y.; Karstens, S. L.; Kwon, H.; Chakraborty, R.; Bustillo, K. C.; Meihaus, K. R.; Furukawa, H.; Minor, A. M.; Head-Gordon, M.; Long, J. R. Selective adsorption of oxygen from humid air in a metal−organic framework with trigonal pyramidal copper(I) sites. *J. Am. Chem. Soc.* **2024**, *146* (5), 3160−3170.

https://doi.org/10.1021/acsengineeringau.5c00051
ACS Eng. Au 2025, 5, 707−725

(109) Solovyeva, M. V.; Gordeeva, L. G.; Krieger, T. A.; Aristov, Yu I. MOF-801 as a promising material for adsorption cooling: Equilibrium and dynamics of water adsorption. *Energy Convers. Manage.* **2018**, *174*, 356−363.
(110) Bezrukov, A. A.; O'Hearn, D. J.; Gascon-Perez, V.; Darwish, S.; Kumar, A.; Sanda, S.; Kumar, N.; Francis, K.; Zaworotko, M. J. Metal-organic frameworks as regeneration optimized sorbents for atmospheric water harvesting. *Cell Rep. Phys. Sci.* **2023**, *4*, No. 101252, DOI: 10.1016/j.xcrp.2023.101252.
(111) Jeremias, F.; Fröhlich, D.; Janiak, C.; Henninger, S. K. Advancement of sorption-based heat transformation by a metal coating of highly-stable, hydrophilic aluminium fumarate MOF. *RSC Adv.* **2014**, *4* (46), 24073−24082.
(112) Swenson, H.; Stadie, N. P. Langmuir's theory of adsorption: A centennial review. *Langmuir* **2019**, *35* (16), 5409−5426.
(113) Chen, S. G.; Yang, R. T. Theoretical basis for the potential theory adsorption isotherms. the Dubinin-Radushkevich and Dubinin-Astakhov equations. *Langmuir* **1994**, *10* (11), 4244−4249.
(114) Sips, R. On the structure of a catalyst surface. *J. Chem. Phys.* **1948**, *16* (5), 490−495.
(115) Luna-Triguero, A.; Sławek, A.; Huinink, H. P.; Vlugt, T. J. H.; Poursaeidesfahani, A.; Vicent-Luna, J. M.; Calero, S. Enhancing the water capacity in Zr-based metal−organic framework for heat pump and atmospheric water generator applications. *ACS Appl. Nano Mater.* **2019**, *2* (5), 3050−3059.
(116) de Lange, M. F.; Verouden, K. J. F. M.; Vlugt, T. J. H.; Gascon, J.; Kapteijn, F. Adsorption-driven heat pumps: The potential of metal−organic frameworks. *Chem. Rev.* **2015**, *115* (22), 12205−12250.
(117) Madero-Castro, R. M.; Luna-Triguero, A.; Sławek, A.; Vicent-Luna, J. M.; Calero, S. On the use of water and methanol with zeolites for heat transfer. *ACS Sustainable Chem. Eng.* **2023**, *11* (11), 4317−4328.
(118) Silva, M. P.; Ribeiro, A. M.; Silva, C. G.; Cho, K. H.; Lee, U.-H.; Faria, J. L.; Loureiro, J. M.; Chang, J.-S.; Rodrigues, A. E.; Ferreira, A. Atmospheric water harvesting on MIL-100(Fe) upon a cyclic adsorption process. *Sep. Purif. Technol.* **2022**, *290*, No. 120803.
(119) Zhang, Z.; Tang, H.; Wang, M.; Lyu, B.; Jiang, Z.; Jiang, J. Metal−organic frameworks for water harvesting: Machine learning-based prediction and rapid screening. *ACS Sustainable Chem. Eng.* **2023**, *11* (21), 8148−8160.
(120) Wang, Y.-M.; Datar, A.; Xu, Z.-X.; Lin, L.-C. In silico screening of metal−organic frameworks for water harvesting. *J. Phys. Chem. C* **2024**, *128* (1), 384−395.
(121) Goeminne, R.; Speybroeck, V. V. Ab initio predictions of adsorption in flexible metal−organic frameworks for water harvesting applications. *J. Am. Chem. Soc.* **2025**, *147* (4), 3615−3630.
(122) Daglar, H.; Gulbalkan, H. C.; Aksu, G. O.; Keskin, S. Computational simulations of metal−organic frameworks to enhance adsorption applications. *Adv. Mater.* **2024**, No. 2405532.
(123) Liu, Z.; Li, W.; Li, S. High-efficiency prediction of water adsorption performance of porous adsorbents by lattice grand canonical Monte Carlo molecular simulation. *RSC Appl. Interfaces* **2025**, *2* (1), 230−242.
(124) Ball, A. K.; Terrones, G. G.; Yue, S.; Kulik, H. J. Data-driven discovery of water-stable metal−organic frameworks with high water uptake capacity. *ACS Appl. Mater. Interfaces* **2025**, *17* (24), 35971−35985.
(125) Dasgupta, S.; Papadimitriou, C. H.; Vazirani, U. V. *Algorithms*; McGraw-Hill Education, 2006.
(126) Huangfu, Qi.; Julian Hall, J. A. Parallelizing the dual revised simplex method. *Math. Program. Comput.* **2018**, *10* (1), 119−142.
(127) Furukawa, H.; Gándara, F.; Zhang, Y.-B.; Jiang, J.; Queen, W. L.; Hudson, M. R.; Yaghi, O. M. Water adsorption in porous metal−organic frameworks and related materials. *J. Am. Chem. Soc.* **2014**, *136* (11), 4369−4381.
(128) Cho, K. H.; Borges, D. D.; Lee, U.-H.; Lee, J. S.; Yoon, J. W.; Cho, S. J.; Park, J.; Lombardo, W.; Moon, D.; Sapienza, A.; Maurin, G.; Chang, J.-S. Rational design of a robust aluminum metal-organic framework for multi-purpose water-sorption-driven heat allocations. *Nat. Commun.* **2020**, *11*, No. 5112, DOI: 10.1038/s41467-020-18968-7.
(129) Lenzen, D.; Zhao, Ji.; Ernst, S.-J.; Wahiduzzaman, M.; Inge, A. K.; Fröhlich, D.; Xu, H.; Bart, H.-J.; Janiak, C.; Henninger, S.; Maurin, G.; Zou, X.; Stock, N. A metal−organic framework for efficient water-based ultra-low-temperature-driven cooling. *Nat. Commun.* **2019**, *10* (1), No. 3025, DOI: 10.1038/s41467-019-10960-0.
(130) Cadiau, A.; Lee, J. S.; Fabry, D. D.; Borges, D.; Fabry, P.; Devic, T.; Wharmby, M. T.; Martineau, C.; Foucher, D.; Taulelle, F.; Jun, C.-H.; Hwang, Y. K.; Stock, N.; De Lange, M. F.; Kapteijn, F.; Gascon, J.; Maurin, G.; Chang, J.-S.; Serre, C. Design of hydrophilic metal organic framework water adsorbents for heat reallocation. *Adv. Mater.* **2015**, *27* (32), 4775−4780.
(131) Wahiduzzaman, M.; Lenzen, D.; Maurin, G.; Stock, N.; Wharmby, M. T. Rietveld refinement of MIL-160 and its structural flexibility upon H_2O and N_2 adsorption. *Eur. J. Inorg. Chem.* **2018**, *2018* (32), 3626−3632.
(132) Hanikel, N.; Pei, X.; Chheda, S.; Lyu, H.; Jeong, W.; Sauer, J.; Gagliardi, L.; Yaghi, O. M. Evolution of water structures in metal-organic frameworks for improved atmospheric water harvesting. *Science* **2021**, *374* (6566), 454−459.
(133) Reinsch, H.; van der Veen, M. A.; Gil, B.; Marszalek, B.; Verbiest, T.; Vos, D. d.; Stock, N. Structures, sorption characteristics, and nonlinear optical properties of a new series of highly stable aluminum mofs. *Chem. Mater.* **2013**, *25* (1), 17−26.
(134) Kiener, C.; Muller, U.; Schubert, M. Organometallic aluminum fumarate backbone material. US Patent US20090092818A1, 2009.
(135) Alvarez, E.; Guillou, N.; Martineau, C.; Bueken, B.; Voorde, B. V. d.; Guillouzer, C. L.; Fabry, P.; Nouar, F.; Taulelle, F.; Vos, D. d.; Chang, J.-S.; Cho, K. H.; Ramsahye, N.; Devic, T.; Daturi, M.; Maurin, G.; Serre, C. The structure of the aluminum fumarate metal−organic framework A520. *Angew. Chem., Int. Ed.* **2015**, *54* (12), 3664−3668.
(136) Wang, S.; Lee, Ji S.; Wahiduzzaman, M.; Park, J.; Muschi, M.; Martineau-Corcos, C.; Tissot, A.; Cho, K. H.; Marrot, J.; Shepard, W.; Maurin, G.; Chang, J.-Sa.; Serre, C. A robust large-pore zirconium carboxylate metal−organic framework for energy-efficient water-sorption-driven refrigeration. *Nat. Energy* **2018**, *3* (11), 985−993.
(137) Iacomi, P.; Formalik, F.; Marreiros, J.; Shang, J.; Rogacka, J.; Mohmeyer, A.; Behrens, P.; Ameloot, R.; Kuchta, B.; Llewellyn, P. L. Role of structural defects in the adsorption and separation of C3 hydrocarbons in Zr-fumarate-MOF (MOF-801). *Chem. Mater.* **2019**, *31* (20), 8413−8423.
(138) Fröhlich, D.; Henninger, S. K.; Janiak, C. Multicycle water vapour stability of microporous breathing mof aluminium isophthalate CAU-10-H. *Dalton Trans.* **2014**, *43* (41), 15300−15304.
(139) Plotdigitizer: Version v3, 2025. https://plotdigitizer.com.
(140) Karloff, H. *Linear programming*; Springer Science & Business Media, 2008.
(141) Dantzig, G. B.; Thapa, M. N. *Linear programming: Theory and extensions*; Springer, 2003; Vol. 2.
(142) Bertsimas, D.; Pachamanova, D.; Sim, M. Robust linear optimization under general norms. *Oper. Res. Lett.* **2004**, *32* (6), 510−516.
(143) Ruszczyński, A.; Shapiro, A.Stochastic programming models. In *Handbooks in Operations Research and Management Science*; Elsevier, 2003; Vol. *10*, pp 1−64.
(144) Nguyen, H. L.; Hanikel, N.; Lyle, S. J.; Zhu, C.; Proserpio, D. M.; Yaghi, O. M. A porous covalent organic framework with voided square grid topology for atmospheric water harvesting. *J. Am. Chem. Soc.* **2020**, *142* (5), 2218−2221.
(145) Sun, C.; Zhu, Y.; Shao, P.; Chen, L.; Huang, X.; Zhao, S.; Ma, D.; Jing, X.; Wang, B.; Feng, X. 2D covalent organic framework for water harvesting with fast kinetics and low regeneration temperature. *Angew. Chem.* **2023**, *135* (11), No. e202217103.
(146) Hu, Y.; Jia, L.; Xu, H.; He, X. Metal−organic framework-assisted atmospheric water harvesting enables cheap clean water

available in an arid climate: A perspective. *Materials* **2025**, *18* (2), No. 379.
(147) Zheng, Z.; Hanikel, N.; Lyu, H.; Yaghi, O. M. Broadly tunable atmospheric water harvesting in multivariate metal−organic frameworks. *J. Am. Chem. Soc.* **2022**, *144* (49), 22669−22675.
(148) Luo, F.; Liao, T.; Liang, X.; Chen, W.; Wang, S.; Gao, X.; Zhang, Z.; Fang, Y. Two-linker MOFs-based glass fiber paper monolithic adsorbent for atmospheric water harvesting in arid climates. *J. Cleaner Prod.* **2022**, *373*, No. 133838.
(149) Gordeeva, L. G.; Tu, Y. D.; Pan, Q.; Palash, M. L.; Saha, B. B.; Aristov, Y. I.; Wang, R. Z. Metal-organic frameworks for energy conversion and water harvesting: A bridge between thermal engineering and material science. *Nano Energy* **2021**, *84*, No. 105946.
(150) Ejeian, M.; Wang, R. Z. Adsorption-based atmospheric water harvesting. *Joule* **2021**, *5* (7), 1678−1703.
(151) Dods, M. N.; Weston, S. C.; Long, J. R. Prospects for simultaneously capturing carbon dioxide and harvesting water from air. *Adv. Mater.* **2022**, *34*, No. 2204277, DOI: 10.1002/adma.202204277.
(152) Lin, H.; Yang, Y.; Hsu, Y.-C.; Zhang, J.; Welton, C.; Afolabi, I.; Loo, M.; Zhou, H.-C. Metal−organic frameworks for water harvesting and concurrent carbon capture: a review for hygroscopic materials. *Adv. Mater.* **2024**, *36* (12), No. 2209073.
(153) Bauer, P.; Thorpe, A.; Brunet, G. The quiet revolution of numerical weather prediction. *Nature* **2015**, *525* (7567), 47−55.
(154) Boretti, A. A perspective for radiative cooling materials. *ACS Appl. Opt. Mater.* **2024**, *2* (6), 991−999.
(155) Elashmawy, M.; Alshammari, F. Atmospheric water harvesting from low humid regions using tubular solar still powered by a parabolic concentrator system. *J. Cleaner Prod.* **2020**, *256*, No. 120329.
(156) Suh, B. L.; Chong, S.; Kim, J. Photochemically induced water harvesting in metal−organic framework. *ACS Sustainable Chem. Eng.* **2019**, *7* (19), 15854−15859.
(157) Park, J.; Yuan, D.; Pham, K. T.; Li, J.-R.; Yakovenko, A.; Zhou, H.-C. Reversible alteration of CO_2 adsorption upon photochemical or thermal treatment in a metal−organic framework. *J. Am. Chem. Soc.* **2012**, *134* (1), 99−102.
(158) Majumdar, A.; Pavone, M. *How Should A Robot Assess Risk? Towards an Axiomatic Theory of Risk in Robotics*; Robotics Research: The 18th International Symposium ISRR; Springer, 2020; pp 75−84.
(159) Gorissen, B. L.; Yanıkoğlu, İ.; Hertog, D. D. A practical guide to robust optimization. *Omega* **2015**, *53*, 124−137.
(160) Wright, A. M.; Kapelewski, M. T.; Marx, S.; Farha, O. K.; Morris, W. Transitioning metal−organic frameworks from the laboratory to market through applied research. *Nat. Mater.* **2025**, *24* (2), 178−187.
(161) Zheng, Z.; Alawadhi, A. H.; Chheda, S.; Neumann, S. E.; Rampal, N.; Liu, S.; Nguyen, H. L.; Lin, Y.-h.; Rong, Z.; Siepmann, J. I.; Gagliardi, L.; Anandkumar, A.; Borgs, C.; Chayes, J. T.; Yaghi, O. M. Shaping the water-harvesting behavior of metal−organic frameworks aided by fine-tuned GPT models. *J. Am. Chem. Soc.* **2023**, *145* (51), 28284−28295.
(162) Hunter, K. M.; Paesani, F. Monitoring water harvesting in metal−organic frameworks, one water molecule at a time. *Chem. Sci.* **2024**, *15* (14), 5303−5310.
(163) Skarmoutsos, I.; Eddaoudi, M.; Maurin, G. Highly efficient rare-earth-based metal−organic frameworks for water adsorption: A molecular modeling approach. *J. Phys. Chem. C* **2019**, *123* (44), 26989−26999.
(164) Rieth, A. J.; Hunter, K. M.; Dincă, M.; Paesani, F. Hydrogen bonding structure of confined water templated by a metal-organic framework with open metal sites. *Nat. Commun.* **2019**, *10* (1), No. 4771.
(165) Nguyen, H. L.; Darù, A.; Chheda, S.; Alawadhi, A. H.; Neumann, S. E.; Wang, L.; Bai, X.; Alawad, M. O.; Borgs, C.; Chayes, J. T.; Sauer, J.; Gagliardi, L.; Yaghi, O. M. Pinpointing the onset of water harvesting in reticular frameworks from structure. *ACS Cent. Sci.* **2025**, *11*, 665−671, DOI: 10.1021/acscentsci.4c01878.
(166) Xie, H.; Atilgan, A.; Joodaki, F.; Cui, J.; Wang, X.; Chen, H.; Yang, L.; Zhang, X.; Son, F. A.; Idrees, K. B.; Wright, A. M.; Wells, J. L.; Morris, W.; Klein, J.; Franklin, L.; Harrington, F.; Herrington, S.; Han, S.; Kirlikovali, K. O.; Islamoglu, T.; Snurr, R. Q.; Farha, O. K. Hydrolytically stable phosphonate-based metal−organic frameworks for harvesting water from low humidity air. *Small* **2025**, *21* (22), No. 2503178.
(167) Xu, J.; Wang, J.; Sheng, X.; Ding, H.; Xu, J.; Chen, S.; Hung, I.; Gan, Z.; Li, Y.; Zhong, J.; Sham, T.-K.; Huang, Y. Unlocking water adsorption mechanisms in Y-BTC mof: Insights from XAFS and SSNMR spectroscopy. *J. Phys. Chem. C* **2025**, *129* (38), 17341−17352.
(168) Terrones, G. G.; Huang, S.-P.; Rivera, M. P.; Yue, S.; Hernandez, A.; Kulik, H. J. Metal−organic framework stability in water and harsh environments from data-driven models trained on the diverse WS24 data set. *J. Am. Chem. Soc.* **2024**, *146* (29), 20333−20348.
(169) Zhang, Z.; Pan, F.; Mohamed, S. A.; Ji, C.; Zhang, K.; Jiang, J.; Jiang, Z. Accelerating discovery of water stable metal-organic frameworks by machine learning. *Small* **2024**, *20* (42), No. 2405087.
(170) Tan, K.; Nijem, N.; Gao, Y.; Zuluaga, S.; Li, J.; Thonhauser, T.; Chabal, Y. J. Water interactions in metal organic frameworks. *CrystEngComm* **2015**, *17* (2), 247−260.
(171) Ai, Q.; Schrier, J. Comment on "environmental stability of crystals: A greedy screening". *Chem. Mater.* **2023**, *35* (2), 801−803.
(172) Yang, Y.; Vayanos, P.; Barton, P. I. Chance-constrained optimization for refinery blend planning under uncertainty. *Ind. Eng. Chem. Res.* **2017**, *56* (42), 12139−12150.
(173) Ohno, H.; Matsubae, K.; Nakajima, K.; Kondo, Y.; Nakamura, S.; Fukushima, Y.; Nagasaka, T. Optimal recycling of steel scrap and alloying elements: Input-output based linear programming method with its application to end-of-life vehicles in Japan. *Environ. Sci. Technol.* **2017**, *51* (22), 13086−13094.
(174) Jamdade, S.; Cai, X.; Allen-Dumas, M. R.; Sholl, D. S. Incorporating diurnal and meter-scale variations of ambient CO_2 concentrations in development of direct air capture technologies. *ACS Sustainable Chem. Eng.* **2024**, *12* (45), 16680−16691.
(175) Cai, X.; Coletti, M. A.; Sholl, D. S.; Allen-Dumas, M. R. Assessing impacts of atmospheric conditions on efficiency and siting of large-scale direct air capture facilities. *JACS Au* **2024**, *4* (5), 1883−1891.
(176) Wiegner, J. F.; Grimm, A.; Weimann, L.; Gazzani, M. Optimal design and operation of solid sorbent direct air capture processes at varying ambient conditions. *Ind. Eng. Chem. Res.* **2022**, *61* (34), 12649−12667.